Neurobiology of Stress 5 (2016) 37–53

Contents lists available at ScienceDirect

Neurobiology of Stress

journal homepage: http://www.journals.elsevier.com/neurobiology-of-stress/

Sex differences in subcellular distribution of delta opioid receptors in the rat hippocampus in response to acute and chronic stress

Sanoara Mazid [a], Baila S. Hall [a, b], Shannon C. Odell [a, b], Khalifa Stafford [a], Andreina D. Dyer [a], Tracey A. Van Kempen [a, b], Jane Selegean [a], Bruce S. McEwen [c], Elizabeth M. Waters [c], Teresa A. Milner [a, b, c, *]

[a] Feil Family Brain and Mind Research Institute, Weill Cornell Medicine, 407 East 61st Street, New York, NY 10065, United States
[b] Weill Cornell Graduate School of Medical Sciences, Weill Cornell Medicine, 1300 York Ave, New York, NY 10021, United States
[c] Harold and Margaret Milliken Hatch Laboratory of Neuroendocrinology, The Rockefeller University, 1230 York Avenue, New York, NY 10065, United States

ARTICLE INFO

Article history:
Received 18 September 2016
Received in revised form
18 October 2016
Accepted 7 November 2016
Available online 10 November 2016

Keywords:
Electron microscopy
CA3 pyramidal cells
GABAergic interneurons
Oxycodone
Neural plasticity
Drug addiction

ABSTRACT

Drug addiction requires associative learning processes that critically involve hippocampal circuits, including the opioid system. We recently found that acute and chronic stress, important regulators of addictive processes, affect hippocampal opioid levels and mu opioid receptor trafficking in a sexually dimorphic manner. Here, we examined whether acute and chronic stress similarly alters the levels and trafficking of hippocampal delta opioid receptors (DORs). Immediately after acute immobilization stress (AIS) or one-day after chronic immobilization stress (CIS), the brains of adult female and male rats were perfusion-fixed with aldehydes. The CA3b region and the dentate hilus of the dorsal hippocampus were quantitatively analyzed by light microscopy using DOR immunoperoxidase or dual label electron microscopy for DOR using silver intensified immunogold particles (SIG) and GABA using immunoperoxidase. At baseline, females compared to males had more DORs near the plasmalemma of pyramidal cell dendrites and about 3 times more DOR-labeled CA3 dendritic spines contacted by mossy fibers. In AIS females, near-plasmalemmal DOR-SIGs decreased in GABAergic hilar dendrites. However, in AIS males, near-plasmalemmal DOR-SIGs increased in CA3 pyramidal cell and hilar GABAergic dendrites and the percentage of CA3 dendritic spines contacted by mossy fibers increased to about half that seen in unstressed females. Conversely, after CIS, near-plasmalemmal DOR-SIGs increased in hilar GABA-labeled dendrites of females whereas in males plasmalemmal DOR-SIGs decreased in CA3 pyramidal cell dendrites and near-plasmalemmal DOR-SIGs decreased hilar GABA-labeled dendrites. As CIS in females, but not males, redistributed DOR-SIGs near the plasmalemmal of hilar GABAergic dendrites, a subsequent experiment examined the acute affect of oxycodone on the redistribution of DOR-SIGs in a separate cohort of CIS females. Plasmalemmal DOR-SIGs were significantly elevated on hilar interneuron dendrites one-hour after oxycodone (3 mg/kg, I.P.) administration compared to saline administration in CIS females. These data indicate that DORs redistribute within CA3 pyramidal cells and dentate hilar GABAergic interneurons in a sexually dimorphic manner that would promote activation and drug related learning in males after AIS and in females after CIS.

1. Introduction

Despite lower rates of drug use and abuse, women are more susceptible to several aspects of drug addiction than men. In particular, women often experience an accelerated course to addiction, shorter-drug free periods and higher levels of craving, and are more likely to relapse due to stressful events or depression (Becker and Hu, 2008; Becker et al., 2007; Fiorentine et al., 1997; Weiss et al., 1997). These processes require associative memory

* Corresponding author. Feil Family Brain and Mind Research Institute, Weill Cornell Medicine, 407 East 61st Street, RM 307, New York, NY 10065, United States.
E-mail addresses: Smsanoarabio@gmail.com (S. Mazid), bah2012@med.cornell.edu (B.S. Hall), sho2004@med.cornell.edu (S.C. Odell), khalifa.stafford89@myhunter.cuny.edu (K. Stafford), adellgunz@gmail.com (A.D. Dyer), tvkempen@gmail.com (T.A. Van Kempen), jselegean@gmail.com (J. Selegean), mcewen@mail.rockefeller.edu (B.S. McEwen), elizabethwaters@mac.com (E.M. Waters), tmilner@med.cornell.edu (T.A. Milner).

http://dx.doi.org/10.1016/j.ynstr.2016.11.002

Abbreviations

ABC	avidin-biotin complex
AIS	acute immobilization stress
BSA	bovine serum albumin
CIS	chronic immobilization stress
CRF	corticotrophin releasing factor
CRF1	corticotrophin releasing factor receptor 1
DAB	diaminobenzidine
DE	diestrus phase
DOR	delta opioid receptor
E	estrus phase
EM	electron microscopy
GABA	gamma aminobutyric acid
IgG	immunoglobulin
ir	immunoreactivity
LM	light microscopy
LTP	long-term potentiation
NPY	neuropeptide Y
PE	proestrus phase
PARV	parvalbumin
PB	phosphate buffer
PBS	phosphate-buffered saline
ROI	region of interest
SIG	silver-intensified immunogold
SOM	somatostatin
TS	tris-buffered saline

and motivational incentives (Koob and Volkow, 2010) that critically involve hippocampal output relayed directly or indirectly to the mesolimbic reward system (Luo et al., 2011; Vorel et al., 2001). This system is a predominant direct target of abused drugs, including opioid receptor agonists, such as the prescription medication oxycodone. Intrinsic hippocampal circuitry supports spatial and episodic memory acquisition processes essential for associating a drug of abuse with a particular place and set of events (i.e., drug-related learning) (Berke and Hyman, 2000; Kilts et al., 2001; Risinger and Oakes, 1995; Volkow et al., 2006). Notably, the opioid system in the CA3 region has been implicated in visual-spatial pattern completion (Kesner and Warthen, 2010), an important component of context associative learning.

Within the hippocampus, the opioid peptide, enkephalin, is contained in the mossy fiber pathway and lateral perforant path (Drake et al., 2007). Enkephalins as well as exogenous opiates (e.g., morphine) predominantly affect excitability and long-term potentiation (LTP) of CA3 pyramidal cells indirectly via activation of μ opioid receptors (MORs) and δ opioid receptors (DORs) which result in inhibition of inhibitory GABAergic interneurons (i.e., disinhibition) (Commons and Milner, 1995; Derrick et al., 1992; Drake et al., 2007; Witter, 1993; Xie and Lewis, 1991). Additionally, enkephalins and exogenous opiates can directly inhibit DORs present on CA3 pyramidal cells (Bao et al., 2007). Our light and electron microscopic studies have demonstrated sex differences in the hippocampal opioid system. Notably, at elevated estrogen states, compared to low estrogen states and males, enkephalins, MORs, and DORs are subcellularly positioned to enhance excitability and learning processes (McEwen and Milner, 2017; Torres-Reveron et al., 2008, 2009; Williams et al., 2011b). Moreover, females in high estrogen states compared to males have a lower baseline transmission in the mossy fiber-CA3 pathway that is regulated by MORs and, unlike males, exhibit a LTP evoked by low frequency stimulation of the mossy fibers that is regulated by DORs.

Drug addiction, particularly relapse, is often provoked by stress (reviewed by (Bruchas et al., 2008; Shalev et al., 2000)). Stress has powerful influences on the addictive processes in both males and females (Koob, 2008). However, females have a heightened sensitivity to stress (Becker et al., 2007) and enhanced cognitive performance following chronic stress (Luine et al., 2007) that may contribute to their accelerated course of addiction, particularly to opioid analgesics (Elman et al., 2001; Hu et al., 2004; Lynch et al., 2000; Robbins et al., 1999). Our recent anatomical studies have shown notable sex differences in the hippocampal opioid system in response to acute and chronic immobilization stress (AIS and CIS, respectively). In particular, our studies suggest that the opioid system of females, regardless of estrogen state, is "primed" for even greater excitation of CA3 pyramidal cells after CIS. After CIS females do not display the atrophy of CA3 pyramidal cell dendrites and the loss of parvalbumin (PARV)-containing GABA interneurons seen in males (McEwen, 1999; Milner et al., 2013; Vyas et al., 2002). Instead, in CIS females, enkephalin levels in mossy fibers are elevated and the subcellular distribution of MORs in hippocampal PARV interneurons resembles that seen in unstressed females at high estrogen states (Milner et al., 2013; Pierce et al., 2014). However, whether DORs also redistribute differently within hippocampal neurons in females and males following AIS and CIS is not known.

Previous light and electron microscopic studies suggest that stress could impact the levels and subcellular distribution of hippocampal DORs in a sexually dimorphic manner (Williams et al., 2011a, 2011b; Williams and Milner, 2011). DOR-immunoreactivity (DOR-ir) is colocalized in neurons containing the stress neurohormone corticotrophin releasing factor (CRF) and its receptor (Williams et al., 2011a; Williams and Milner, 2011). Our electron microscopic studies have demonstrated that females in high estrogen states exhibit internalization and trafficking of DORs towards the soma of CA1 pyramidal cells; this is not seen in females in low estrogen states in males (Williams et al., 2011b). Moreover, females at high estrogen states have elevated levels of phosphorylated DORs in CA2/3 pyramidal cells compared to females at low estrogen states and males, which then is reduced following AIS (Burstein et al., 2013). As DOR phosphorylation parallels the uncoupling and internalization of DORs (Pradhan et al., 2009), this suggests that CA2/3 neurons in females at high estrogen states may be more sensitive to opioid agonists.

Thus, this study sought to determine the levels and trafficking of DORs in the hippocampus following stress, and further if this differs in females and males. For this, dual labeling electron microscopic immunocytochemistry examined the distribution of DORs in CA3 pyramidal cells and GABAergic interneurons in the dentate hilus after AIS and CIS.

2. Materials and methods

2.1. Animals

All procedures were approved by the Rockefeller University and Weill Cornell Medicine Institutional Animal Care and Use Committees and were in accordance with the 2011 Eighth edition of the National Institutes of Health guidelines for the Care and Use of Laboratory Animals. Adult male (~275–325 gm) and female

(~225–250 gm) Sprague-Dawley rats (N = 104; Charles River Laboratories, Wilmington, MA) were approximately 2 month old at the time of arrival. The rats were pair-housed with 12:12 light/dark cycles (Lights on 0600–1800) and had access to food and water *ad libitum*. The rats used in this study were the same as those used in our previous studies (Burstein et al., 2013; Gonzales et al., 2011; Milner et al., 2013; Pierce et al., 2014).

2.1.1. Estrous cycle determination

Only female rats that showed two consecutive, regular 4–5 day estrous cycles prior to initiation of AIS or CIS were used. Estrous cycle stage was determined using vaginal smear cytology (Turner and Bagnara, 1971) daily between 9:00 and 10:00 a.m., following 1 week of acclimation after arrival. To control for the effects of handling, males were removed from their cages daily and mock estrous cycling was performed. Previous studies (Milner et al., 2013) confirmed estrous cycle stages in these same rats using uterine weight and plasma serum estradiol levels via radioimmunoassay were measured. Three estrous cycle stages were chosen for study: proestrus (elevated estrogen levels, 0.5–1 day long), estrus (declining estrogen levels, 2–2.5 days long) and diestrus 2 rats (referred to here as diestrus, low estrogen and progestin levels, 2–2.5 days long). Previous studies in these rats showed that CIS had no effect on the length of the estrous cycle or the duration of the individual estrous phases (Milner et al., 2013).

2.1.2. Acute immobilization stress

Rats (N = 48) were transported from their home-room into a procedure room between 9:00 a.m. and 1:00 p.m., and AIS was performed as previously described (Lucas et al., 2007; Shansky et al., 2010). Briefly, rats were placed in plastic cone-shaped polyethylene bags with a small breathing hole at the apex and a Kotex mini-pad was placed underneath them to collect urine. The rats were placed with their nose at the hole and the bag was sealed with tape; they then were left undisturbed on the countertop for 30 min. Immediately after the conclusion of the AIS, the rats were anesthetized in a neighboring procedure room and their brains fixed via perfusion (see below). Control rats were left in the home-room and anesthetized prior to transfer to the procedure room for perfusion.

2.1.3. Chronic immobilization stress

During the stress paradigm, the control and CIS rats were pair-housed in separate rooms. For CIS, the rats (N = 48) were subjected to the AIS procedure as described above for 10 consecutive days. Rats were killed 24 h after the final stress period.

2.1.4. Acute oxycodone administration

In a separate cohort, 8 female rats were subjected to CIS as described in Section 2.1.3. Twenty-three hours later, four control and four CIS female rats were injected with 3 mg/kg (I.P) of oxycodone. This dose of oxycodone was chosen because it induces conditioned place preference in young adult female Sprague Dawley rats (Olmstead and Burns, 2005). The rats were killed one hour later. Estrous cycle assessment at the termination of the experiment showed that the rats were in estrus.

2.2. Immunocytochemistry procedures

2.2.1. Section preparation

Rats were deeply anesthetized with sodium pentobarbital (150 mg/kg, I.P.) and perfused sequentially through the ascending aorta with: (1) 10–15 ml 0.9% saline containing 2% heparin; (2) 50 ml of 3.75% acrolein and 2% paraformaldehyde in 0.1 M phosphate buffer (PB; pH 7.4); and (3) 200 ml of 2% paraformaldehyde in PB (Milner et al., 2011). After the perfusion, brains were removed from the skull, cut into 5 mm coronal blocks, postfixed in 2% paraformaldehyde in PB for 30 min, and then transferred into PB. Coronal sections (40 μm thick) through the hippocampus were cut on a vibrating microtome (Leica Microsystems, Buffalo Grove, IL) into PB. Sections were stored in cryoprotectant solution (30% sucrose and 30% ethylene glycol in PB) at 20 °C.

Prior to immunocytochemistry, one section per rat from the dorsal hippocampus [-3.5 to −4.2 mm from Bregma (Swanson, 1992)] was rinsed in PB. To ensure identical labeling conditions between experimental groups for quantitative immunocytochemistry (Pierce et al., 1999), the sections were coded with hole-punches, pooled into single containers and then processed together through all immunocytochemical procedures. The sections were incubated in 1% sodium borohydride in PB for 30 min to neutralize reactive aldehydes (Milner et al., 2011) and rinsed thoroughly in PB.

2.2.2. Antibody characterization

2.2.2.1. DOR. A rabbit polyclonal antibody against amino acids 3–17 of the DOR (AB1560, Millipore, Temecula, CA) was used for these studies. In lysates from whole rat brain, cerebral cortex, hippocampus and spinal cord, and in NG108-15 cells, which have been shown to endogenously express DORs (Barg et al., 1984; Kieffer et al., 1992; Persson et al., 2005), Western blots for AB1560 yield two major bands at 36kD and 72kD [see Supplemental Fig. 1 in (Williams et al., 2011a) and (Persson et al., 2005; Saland et al., 2005)]; moreover, rat spinal cord lysates have an additional 48kD band on Western blots (Persson et al., 2005). The 72 kDa band is thought to represent a dimer or a glycosylated form of DOR (Persson et al., 2005; Saland et al., 2005). In rat whole rat brain lysates, cerebral cortex and spinal cord, the 36kD, 48kD and 72kD bands were partly blocked after 1 h preincubation of the AB1560 antibody with 10 μg/ml of the immunogenic peptide and completely eliminated after 1 h preincubation of the AB1560 antibody with 150 μg/ml of immunogenic peptide (Persson et al. 2000, 2005). Moreover, no detectable labeling of this antibody is seen in Western blots of COS-7 cells (see Supplemental Fig. 1 in Williams et al., 2011a) that do not endogenously express DORs (Kieffer et al., 1992).

Preadsorption of a 1:100 dilution of AB1560 with the synthetic epitope sequence of DOR1 3–17 at 10^{-4} M overnight at 4 °C nearly eliminated immunofluorescent labeling in the rat striatal sections fixed with 4% paraformaldehyde (Olive et al., 1997). A 1:250 dilution of AB1560 labeled cells in paraformaldehyde-fixed sections from the dorsal raphe of wild-type mice but not DOR knockout mice (The Jackson Laboratory, B6.129S2-Oprd1tm1) as determined by immunofluorescence (see Supplemental Fig. 1 in Bie et al., 2010). [However, the pattern of immunofluorescent labeling of AB1560 did not differ in 10% formalin-fixed spinal cord sections from wildtype and DOR knock-out mice (see Supplementary Fig. 5, in Scherrer et al., 2009).] Controls omitting the AB1560 antiserum and processed for peroxidase labeling did not result in any labeling in rat hippocampal acrolein-paraformaldehyde fixed sections (Commons and Milner, 1997).

The DOR AB1560 antibody has been previously characterized for light and electron microscopic studies in the rat hippocampus (Commons and Milner, 1996a, 1997; Williams et al., 2011a, 2011b; Williams and Milner, 2011). Our previous studies have shown that DOR immunoreactivity in the rat hippocampus is fixation sensitive and yields the most intense labeling with 3.75% acrolein and 2% paraformaldehyde fixed sections compared to 4% paraformaldehyde fixed sections (Commons and Milner, 1997). In the rat hippocampus, the pattern of DOR-labeling seen at the light microscopic level as well as the types and distribution of DOR-labeled profiles seen at the electron microscopic level are

identical with AB1560 and a polyclonal guinea pig antiserum raised against amino acids 34–48 (p34) of the mouse DOR (Commons and Milner, 1996b, 1997). Moreover, the pattern of DOR-immunolabeling in the rat hippocampus seen with these two antibodies is consistent with that seen for DOR mRNA expression in the rat, which indicated that interneurons have higher levels of DOR expression than pyramidal cells (Mansour et al., 1994). The distribution of DOR-immunoreactivity in the rat hippocampus also is in agreement with the distribution of DOR binding sites in the rat hippocampus described previously by autoradiography (Crain et al., 1986; Gulya et al., 1986; Mansour et al., 1987; McLean et al., 1987).

2.2.2.2. GABA. A rat polyclonal antiserum was produced against GABA-glutaraldehyde-hemocyanin conjugates, and was provided by A. Towle, formerly affiliated with Dept. of Neurology at Cornell University Medical College. The specificity of this antiserum was tested using preadsorption with GABA-bovine serum albumin (BSA), which eliminated immunoreactivity; however, preadsorption with unconjugated GABA or BSA conjugated to glutamate, β-alanine or taurine did not abolish immunoreactivity (Lauder et al., 1986). Additionally immunoreactivity of this antiserum has been reported to be consistent with the specificity of other GABA-antisera (Lauder et al., 1986).

2.2.2.3. Neuropeptide Y (NPY). The rabbit polyclonal antibody against porcine NPY was obtained from Peninsula Laboratories International (San Carlos, CA). On immunodot blots, this antibody recognizes a 10^{-8} M concentration of NPY and closely related peptides YY and pancreatic polypeptide at 10^{-5} M concentrations (Milner and Veznedaroglu, 1992). This antibody has been used in previous light and electron microscopic studies (Ledoux et al., 2009; Milner and Veznedaroglu, 1992; Milner et al., 1997; Rogers et al., 2016).

2.2.3. Light microscopic immunocytochemistry

To examine changes in the density of DOR-ir in the hippocampus In the AIS and CIS groups, sections were processed using previously described methods (Williams et al., 2011b). Briefly, sections were rinsed in 0.1 M Tris-buffered saline (TS; pH 7.6) and then blocked in 0.5% BSA in TS for 30 min. Sections were incubated in rabbit anti-DOR antibody (1:5000 dilution) made in 0.1% BSA and TS for 1 day at room temperature, and then 1 day at 4 °C. Sections then were incubated in a 1:400 dilution of biotinylated donkey-anti-rabbit immunoglobulin (IgG; Jackson Immunoresearch Laboratories, Westgrove, PA) for 30 min followed by 1:100 dilution of avidin–biotin complex (ABC; Vectastain elite kit, Vector Laboratories, Burlingame, CA) for 30 min. All incubations were separated by washes of TS. Sections were reacted in 2,2- diaminobenzidine (DAB; Sigma-Aldrich, St. Louis, MO) and 3% H_2O_2 in TS for 6 min and in TS followed by PB. Sections were mounted on gelatin-coated slides, dehydrated, and coverslipped from xylene with DPX mounting media (Sigma-Aldrich).

To determine if the numbers of NPY-containing cells, which are known to colocalize DOR (Drake et al., 2007), were altered following CIS, sections from the diestrus females and males were processed for peroxidase immunolabeling as described above. In this experiment, the NPY antibody was diluted 1:15,000 in 0.25% triton in 0.1% BSA and TS.

2.2.4. Dual labeling electron microscopic immunocytochemistry

Sections were dually labeled for DOR and GABA using a previously described protocol (Milner et al., 2011). In brief, sections were incubated in a combination of the rabbit DOR antibody (1:5000 dilution) and the rat GABA antibody (1:1000 dilution) in 0.1% BSA and TS for 1 day at room temperature and 4 days at 4 °C. Sections then were processed for peroxidase labeling for GABA as described for light microscopy (sec. 2.2.3), except that a secondary donkey anti-rat IgG conjugated to biotin (Jackson Labs) was used. Next, sections were rinsed in TS and incubated in donkey anti-rabbit IgG conjugated to 1 nm gold particles (1:50 dilution; Electron Microscopy Sciences (EMS), Fort Washington, PA) in 0.01% gelatin and 0.08% BSA in 0.01 M phosphate-buffered saline (PBS; pH 7.4) at 4 °C overnight. Sections were rinsed in PBS, postfixed in 2% glutaraldehyde in PBS for 10 min, and rinsed in PBS followed by 0.2 M sodium citrate buffer (pH 7.4). The conjugated gold particles were enhanced by reaction in a silver solution (RPN491 Silver Enhance kit, GE Healthcare, Waukeska, WI) for 6 min. Sections then were rinsed thoroughly in PB.

Sections were fixed in 2% osmium tetroxide for 1 h followed by PB rinses and dehydration in increasing concentrations of ethanol and propylene oxide before being embedded in EMbed 812 (EMS) (Milner et al., 2011). Ultrathin sections (70–72 nm thick) were cut from the CA3b region or dentate gyrus on a Leica UCT ultratome and collected on 400 mesh thin-bar copper grids (EMS). The grids were counterstained with uranyl acetate and Reynolds lead citrate.

2.3. Data collection and analysis

All people who performed all data collection and analyses were blinded to experimental condition. Data were unblinded after the final graphs were generated.

2.3.1. Light microscopy

Quantitative densitometric analysis of DOR-ir of regions of interest (ROI) in the hippocampus of rats from the AIS and CIS groups was determined using previously described methods (Pierce et al., 2014; Williams et al., 2011b). For this, images of the hippocampus were captured with a 4× objective on a Nikon Eclipse 80i microscope using a Dage MTI CCD-72 camera and MicroComputer Imaging Device (MCID; Linton, UK) software. Blank fields taken from a slide without tissue first were subtracted to compensate for uneven illumination across the field. For each captured image, average pixel densities (out of 256 gray levels) were then determined using NIH ImageJ software for stratum radiatum in CA3b. To compensate for background staining levels and to control for variations in the overall illumination level between images, the average pixel density for three small regions lacking labeling (white matter) was subtracted. Optical density was measured using ImageJ64.

The number of DOR- or NPY-labeled was determined in the hilus of the dentate gyrus from the males and females (estrus stage only) in the CIS group as previously described (Milner et al., 1997; Williams et al., 2011b). Using the granule cell layer as a border, all labeled cells (DOR or NPY) with a distinguishable nucleus were counted in the hilus excluding cells in the CA3 cell layer border. The area of the hilus was determined using ImageJ64 software. The number of cells per unit area of the hilus then was calculated. In addition to this analysis, the number of cells in the crest, central hilus and dorsal blade of the hilus was determined. For this, a 200-μm^2 rectangle was placed over these regions using the granule cell layer as a guide.

2.3.2. Electron microscopy

Sections from the CA3b and hilus of the dentate gyrus were examined on CM10 transmission electron microscope (FEI, Hillsboro, OR). Images were collected at a magnification of 13,500. Profiles were identified and categorized as neuronal (soma, dendrites, axons, terminals) or glial based on standardized morphological characteristics (Peters et al., 1991). Dendritic profiles contained regular microtubular arrays and were usually postsynaptic to axon terminal profiles. Dendritic profiles were further

classified as large (average diameter >1.0 μm) and small (average diameter <1.0 μm). Axon terminal profiles had numerous small synaptic vesicles and had a cross-sectional diameter greater than 0.2 μm. Mossy fiber terminals were identified by their large size (~1–1.5 μm in diameter), irregular contour and presence of numerous small synaptic vesicles (Amaral and Dent, 1981).

Immunoperoxidase labeling for GABA was distinguished as an electron-dense reaction product precipitate. Silver intensified immunogold (SIG) labeling for DOR appeared as black electron-dense particles that varied in size. Occasionally, SIG particles were clustered together (e.g., Fig. 2A). In these instances, the SIG particle was counted as one. Although sometimes DAB precipitate appeared as dots, it was not black and clearly distinguishable from the SIG particles. To minimize false negative labeling of smaller profiles, profiles were considered as dual-labeled if they contained electron-dense reaction product and at least one gold particle. Criteria for field selection included good morphological preservation, the presence of immunolabeling in the field, and proximity to the plastic–tissue interface (i.e., the surface of the tissue) to avoid problems due to differences in antibody penetration (Milner et al., 2011).

For the analysis, DOR-SIG particle localization was recorded as, plasmalemmal, near plasma membrane (i.e., particles within 50 nm, but not touching the plasma membrane) or cytoplasmic. The presence of plasmalemma receptors identified by SIGs corresponds to sites of receptor binding (Boudin et al., 1998). Receptors may be inserted into or removed from the plasmalemma from a pool of receptors near the plasmalemma. Cytoplasmic receptors may be stored, in transit to/from the cell body or other cellular compartments, as well as in the process of being degraded or recycled (Fernandez-Monreal et al., 2012; Pierce et al., 2009). In response to agonist stimulation, the ratio of plasmalemma-to-cytoplasmic SIG labeled receptors shows the expected decrease (Haberstock-Debic et al., 2003). Thus, the distribution of protein as identified by SIGs likely reflects receptor functionality.

2.3.2.1. Analysis 1: DOR-SIG labeling in CA3 and the dentate gyrus. Micrographs containing single SIG DOR labeled dendrites were collected from stratum radiatum of CA3 or dual labeled dendrites from the hilus of the dentate gyrus as previously described (Milner et al. 2011, 2013). For this, 50 labeled dendritic profiles were randomly selected from the tissue-plastic interface and photographed. Usually, one thin section per block was sufficient to obtain the required number of profiles. Occasionally two sections per block were analyzed. In this case, the profiles were taken from non-overlapping regions of the block. The subcellular distribution and density of DOR-SIG particles in GABA-labeled dendrites was determined as previously described (Williams et al., 2011b). For this, Microcomputer Imaging Device software (MCID, Imaging Research Inc., Ontario, Canada) was used to determine perimeter (i.e., plasmalemma), cross-sectional area, average cross-sectional diameter, and major and minor axis lengths of each immunolabeled dendrite. Dendrites with an oblong or irregular shape (form factor value < 0.5) were excluded from the data set. The parameters used for statistical comparisons were: 1) the number of plasma membrane DOR-SIG particles on the dendrite perimeter (PM:μm); 2) the number of near plasma membrane DOR-SIG particles per perimeter (Near:μm); 3) the number of cytoplasmic DOR-SIG particles per cross-sectional area (CY:μm^2); and 4) the total number of DOR-SIG particles (sum of plasmalemmal, near-plasmalemmal and cytoplasmic) in a dendritic profile/unit cross-sectional area (Total:μm^2). The partitioning ratio is the proportion of DOR-SIG particles in a particular subcellular compartment (e.g., plasma membrane or cytoplasm) divided by the total number of DOR-SIG-particles. Dendrites were divided further into large (>1.0 μm) and small (≤1.0 μm) based on average diameter, which correspond to proximal and distal to the cell body (Peters et al., 1991).

2.3.2.2. Analysis 2: DOR-SIG labeling in spines contacted by mossy fibers. The analysis was similar to that described previously (Harte-Hargrove et al., 2015). Fifty mossy fiber profiles per rat were collected from random fields of stratum lucidum of CA3b near the tissue-plastic interface from each block. All spine profiles that were in contact with a mossy fiber profile were counted and classified as DOR-labeled (i.e., containing at least 1 SIG particle) or non-DOR labeled. DOR-SIG particles in dendritic spines were then classified as on the plasma membrane or synapse or in the cytoplasm.

2.4. Statistical analysis and figure preparation

Data are expressed as means ± SEM. Statistical relationships were examined with a student' *t*-test or with analysis of variance (ANOVA) with Tukey's post-hoc tests through JMP11 software (SAS Institute, Inc.). Values were considered statistically significant when $p < 0.05$.

Adjustments to brightness, contrast and sharpness were made in Adobe Photoshop 9.0 on an iMac prior to importing into PowerPoint 2010, where final adjustments to brightness, contrast and size were made. These changes did not alter the original content of the raw image. Graphs were generated in Prism 6.

3. Results

3.1. Sex, cycle phase and duration of stress differentially alter DOR levels in CA3b

Consistent with previous light microscopic descriptions of DOR-labeling in CA3 (Commons and Milner, 1997; Williams et al., 2011b), DOR-ir was in the CA2 and CA3 pyramidal cell layers (Fig. 1A and B). Moreover, DOR-ir was diffusely distributed in stratum radiatum and, to a greater extent, in stratum lucidum (Fig. 1B). A few scattered DOR-immunoreactive interneurons also were observed in stratum oriens (Fig. 1A).

As previous studies have shown sex and estrus cycle phase affect the levels of DOR-ir in CA1 (Williams et al., 2011b), we analyzed the levels of DOR-ir in stratum radiatum of CA3b for effect of cycle phase (proestrus, estrus, diestrus), sex and stress (stress or control) using a two-way ANOVA. In the AIS group, there were significant main effects of cycle [$F(3,26) = 12.81$, $P < 0.0001$] and stress [$F(1,26) = 28.34$, $P < 0.0001$], but no significant interaction of cycle and stress [$F(3,26) = 0.3546$, $P = 0.7862$). In the CIS group, there was a significant main effect of cycle [$F(3,32) = 3.647$, $P = 0.0228$] but no significant main effect of stress [$F(1,32) = 0.580$, $P = 0.1180$]. In both the AIS and CIS control groups, post-hoc analyses demonstrated that the levels of DOR-ir were significantly less ($p < 0.05$) in proestrus females compared to diestrus females (Fig. 1C and D).

Post-hoc analyses showed that AIS and CIS had the opposite effect on the levels of DOR-ir in stratum radiatum of CA3b in females and males. Following AIS, the levels of DOR-ir were significantly reduced ($p < 0.05$) in both proestrus females and males, but not estrus and diestrus females (Fig. 1C). However, the levels of DOR-ir in proestrus rats compared to diestrus rats were still significantly lower ($p < 0.05$) after AIS (Fig. 1C). In contrast, CIS significantly elevated DOR-ir in proestrus females and significantly lowered ($p < 0.05$) DOR-ir levels in diestrus females. Moreover, CIS did not significantly affect the levels of DOR-ir in males (Fig. 1D). Thus, CIS eliminated the influence of cycle phase on DOR levels and essentially shifted the DOR levels to the middle levels observed in estrus control rats.

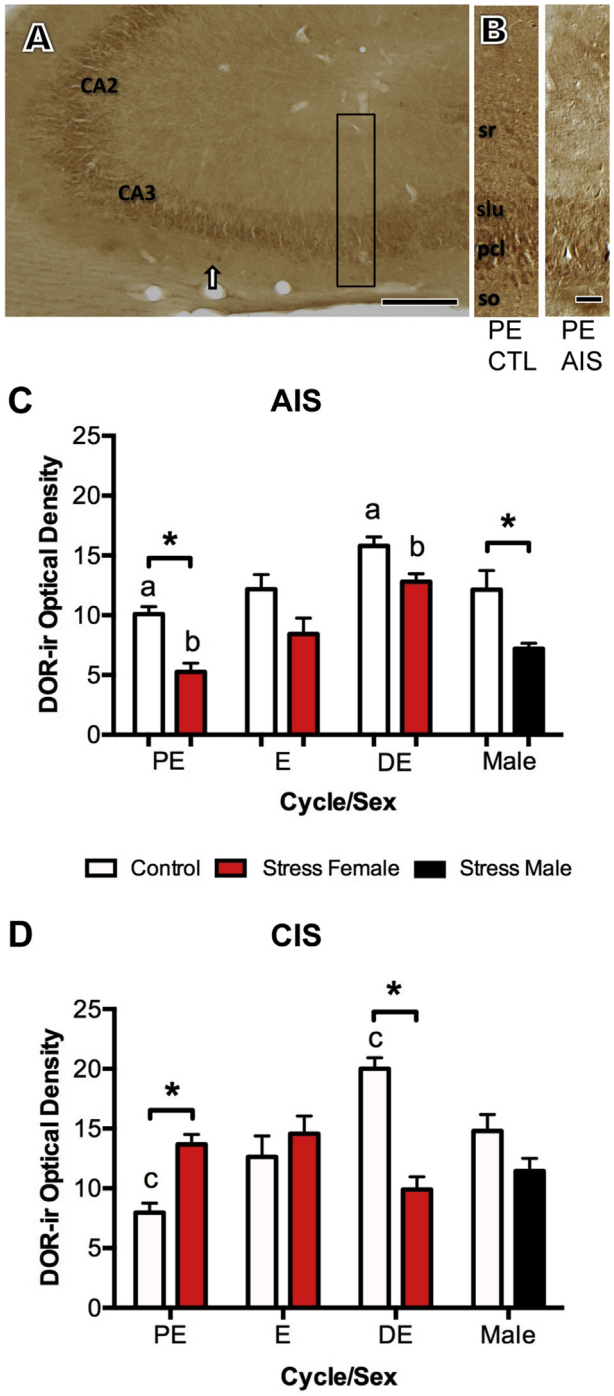

Fig. 1. Effects of estrous cycle phase and sex on the levels of DOR-ir in the CA3 region. **A**. Low magnification photomicrograph shows DOR-ir is in the CA2 and CA3 regions from the dorsal hippocampus of a diestrus rat. Arrow indicated example of DOR-labeled neurons in stratum oriens. Box shows region of CA3b sampled for densitometry. **B**. Higher magnification of CA3b shows representative DOR-labeling from proestrus (PE) control and AIS females. The levels of DOR-ir were sampled in stratum radiatum (sr). pcl, pyramidal cell layer, slu, stratum lucidum, so, stratum oriens. Scale bars A = 100 μm; B = 100 μm. **C and D**. In control rats, the levels of DOR-ir were significantly elevated (a, c; $p < 0.05$) in CA3 stratum radiatum in diestrus (DE) rats compared to proestrus rats. **C**. AIS significantly decreased (*$p < 0.05$) the levels of DOR-ir in CA3 stratum radiatum in proestrus females and males. Following AIS, the levels of DOR-ir in diestrus rats were elevated compared to proestrus rats (b: $p < 0.05$). **D**. Following CIS, fluctuations in DOR-ir in CA3 stratum radiatum over the estrus cycle in females were not apparent and the levels of DOR-ir significantly increased (*$p < 0.05$) in proestrus females and significantly decreased (*$p < 0.05$) in diestrus females. N = 6 animals per group.

3.2. Baseline densities of DOR in CA3b dendrites differ in proestrus females and males

The cycle stage in which the greatest difference in DOR levels by light microscopy was observed was chosen for EM analysis. Thus, proestrus and diestrus rats were analyzed following AIS and CIS, respectively. In both females and males, DOR-SIG particles were on the plasma membrane, near the plasma membrane and in the cytoplasm of dendritic shafts in stratum radiatum of CA3b (Fig. 2A and B). Consistent with previous studies (Commons and Milner, 1996a), DOR-labeling also was detected in terminals, axons and glia (not shown).

Initially, the baseline density of DOR-SIG particles in dendritic shafts was determined by comparing the control female and male from the AIS groups using a student t-test. The control female rats from the AIS group had significantly more near plasma membrane DOR-SIG particles than control males ($t_{246.8} = -2.75$, $p = 0.0064$) from the AIS group (Fig. 3A). Similarly, the control female rats showed increased partitioning ratio near plasmalemma ($t_{262.4} = -2.52$, $p = 0.0122$) as well as in the cytoplasm ($t_{262.4} = 2.53$, $p = 0.0121$). A similar analysis comparing DOR labeling in control CIS diestrus females with males showed no significant differences between the two groups (not shown). Thus, at baseline, proestrus females have a greater proportion of DORs poised to be inserted into the plasma membrane of CA3 pyramidal cell dendrites.

3.3. AIS and CIS have opposite effects on the distribution of DORs in CA3 dendrites in females and males

No differences in the density of plasmalemmal, near plasmalemmal, cytoplasmic or total DOR-SIG particles in CA3 dendrites in either female or male rats were seen following AIS (Fig. 3C and D). However, when CA3 dendrites were analyzed by size, significant differences emerged: there was a significant increase in the cytoplasmic density ($t_{123.8} = -2.11$, $p = 0.0371$) of DOR-SIG particles in large dendrites of the females after AIS (Figs. 2A,C and 3F) and a significant increase in the density of near plasmalemmal ($t_{102.2} = -2.35$, $p = 0.0210$) and total ($t_{104.9} = -2.30$, $p = 0.0234$) DOR-SIG particles in small dendrites in males after AIS (Figs. 2B,D and 3F).

CIS had the opposite effects of AIS on the distribution of DOR-SIG particles in CA3 dendrites in females and males. After CIS, there was a significant decrease in the cytoplasmic ($t_{271.5} = 5.49$, $p < 0.0001$) and total ($t_{251.2} = 5.66$, $p < 0.0001$) density of DOR-SIG particles in females (diestrus) (Fig. 4A, B & E). In males, CIS decreased the density of DOR-SIG particles on the plasma membrane ($t_{88.4} = 2.81$, $p = 0.0061$) of CA3 dendrites (Fig. 4C, D and F). Further analysis showed that the partitioning ratio of DOR-SIG particles in CA3 dendrites was not different in females after CIS in any cellular compartment (Fig. 4G). However, the partitioning ratio of DOR-SIG particles on the plasma membrane of CA3 dendrites was significantly decreased ($t_{104.3} = 2.31$, $p = 0.0231$) in the males after CIS (Fig. 4H).

As our previous studies have shown that the percent of DOR labeled spines contacted by mossy fibers is greater in proestrus females compared to males (Harte-Hargrove et al., 2015), we next analyzed the effect of AIS and CIS on the percent of DOR labeled spines contacted by mossy fibers. AIS had no significant effect on the percent of DOR-labeled spines in proestrus females but significantly increased ($t_{3.24} = 3.42$, $p = 0.0371$) the percent of DOR labeled spines in males (Fig. 5A–C). Following CIS, only dendritic spines in females were analyzed as previous studies in males have shown that CIS results in a loss of CA3 pyramidal cell dendritic spines (McEwen, 1999). Following CIS, the percentage of dendritic

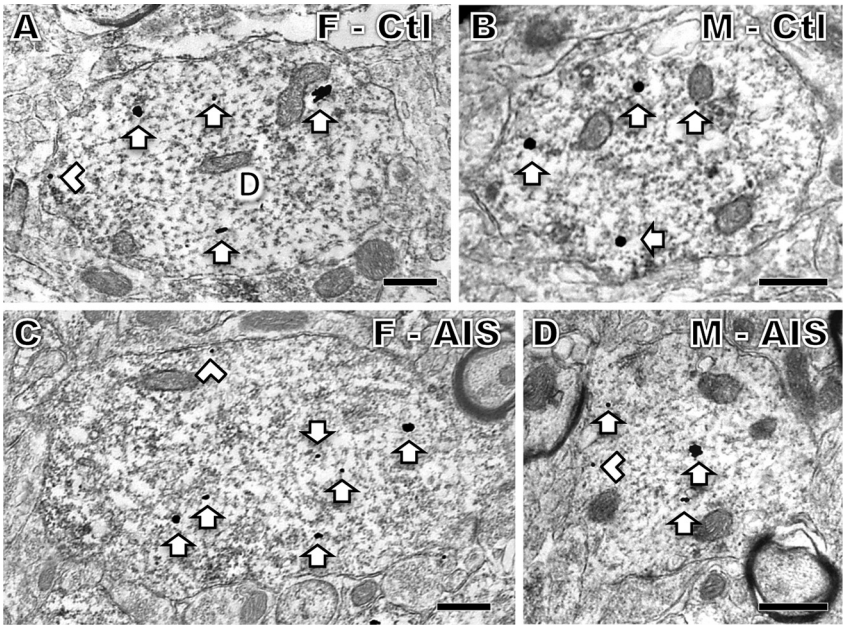

Fig. 2. Representative electron micrographs of DOR-SIG labeling in CA3 pyramidal cell dendrites from females and males after AIS. A. Control proestrus female. **B**. Control male. **C**. AIS proestrus female. **D**. AIS male. Examples of near plasmalemmal (chevron) and cytoplasmic (arrow) DOR-SIG particles in dendrites (D) are shown. After AIS, cytoplasmic DOR-SIG particles are elevated in females and near plasmalemmal particles are elevated in males. Scale bars A - D = 500 nm.

spines that contacted mossy fibers approached a significant decrease ($t_{2.3} = 3.68$, $p = 0.0530$; Fig. 5D).

Thus, in females cytoplasmic pools of DORs increase after AIS but decrease after CIS. Conversely, in males DORs traffic towards the plasma membrane of CA3 dendrites and spines after AIS but traffic away from the plasma membrane after CIS.

3.4. CIS increases the number of DOR-labeled cells in a select hilar subregion in females

Previous studies have shown that subpopulations of hilar GABAergic interneurons coexpress different opioid receptors: MORs are predominant on PARV interneurons whereas DORs are predominant on NPY/somatostatin (SOM) containing interneurons in rats (reviewed in (Drake et al., 2007)). Chronic stress decreases the number of PARV-containing neurons in the hilus of the dentate gyrus of male but not female rats (Hu et al., 2010; Milner et al., 2013). While it is unknown if CIS affects the number of DOR-containing neurons in the hilus, this is important as it would impact the interpretation of the EM assessment of DOR redistribution in GABAergic interneurons after CIS.

Consistent with previous studies (Commons and Milner, 1996a; Williams and Milner, 2011), DOR-labeled interneurons were located in the dorsal blade, central and crest regions of the hilus (Fig. 6A). DOR-labeled neurons were rarely found in the subgranular region of the hilus. After CIS, the total number of DOR-labeled neurons increased in the females ($t_{7.14} = -2.61$; $p = 0.0343$; Fig. 6C) but was not altered in the males (Fig. 6E). Further analysis of the hilar subregions showed that CIS selectively increased the number of DOR-labeled cells in the dorsal blade of females ($t_{8.71} = -2.65$; $p = 0.0273$; Fig. 6B,D) but did not significantly alter the number of DOR-labeled cells in the males (Fig. 6F).

Like DOR, NPY-labeled neurons in the dentate hilus were located in the dorsal blade, central and crest regions of the hilus (Suppl. Fig. 1). There were no significant differences in the total number of NPY-labeled neurons in the females after CIS (Suppl. Fig. 1C). However, the total number of NPY-labeled neurons decreased in the males (Suppl. Fig. 1A,B and D). Neither females nor males had significant differences in the hilar subregions (not shown).

3.5. AIS and CIS have the opposite effect on the redistribution of DORs in hilar GABAergic interneurons in females and males

In all groups, dendrites dually labeled for DOR and GABA were sampled from the central and crest subregions of the hilus. Similar to previous observations (Commons and Milner, 1996a), dual labeled dendrites were primarily observed in the central hilar region. Dual labeled dendrites lacked dendritic spines and were often contacted by several axon terminals that formed asymmetric synapses (Figs. 7A–D and 8A–D).

As observed in the CA3 region, AIS did not alter the density of DOR-SIG particles in GABA-labeled dendrites in any cellular compartment in either females or males (Fig. 7E and F). However, when separated by dendritic size, significant differences in the redistribution of DOR-SIG particles emerged and these were sexually dimorphic. After AIS, the density of near plasma membrane DOR-SIG particles in large GABA-labeled dendrites significantly decreased in females ($t_{100.97} = 2.43$, $p = 0.0170$; Fig. 7A, B & G). In contrast, AIS significantly increased ($t_{123.2} = 2.15$, $p = 0.029$) the density of near plasma membrane DOR-SIG particles in small GABA-labeled dendrites in males (Fig. 7C,D & H).

The pattern of redistribution of DOR-SIG particles seen following CIS in females compared to males is the opposite as that observed after AIS. After CIS, no significant differences in the density of DOR-SIG particles in GABA-labeled dendrites were seen in any cellular compartment in either females or males (Fig. 8E and F). However, there were significant sex differences in the partitioning ratio of DOR-SIG particles in GABA-labeled dendrites after CIS. The proportion of DOR-SIG particles on the near plasma membrane compartment significantly increased ($t_{372.7} = -2.18$, $p = 0.0299$) in females (Fig. 8A,B & G) and tended to decrease ($t_{320.4} = 1.89$, $p = 0.0600$) in the males (Fig. 8C,D & H).

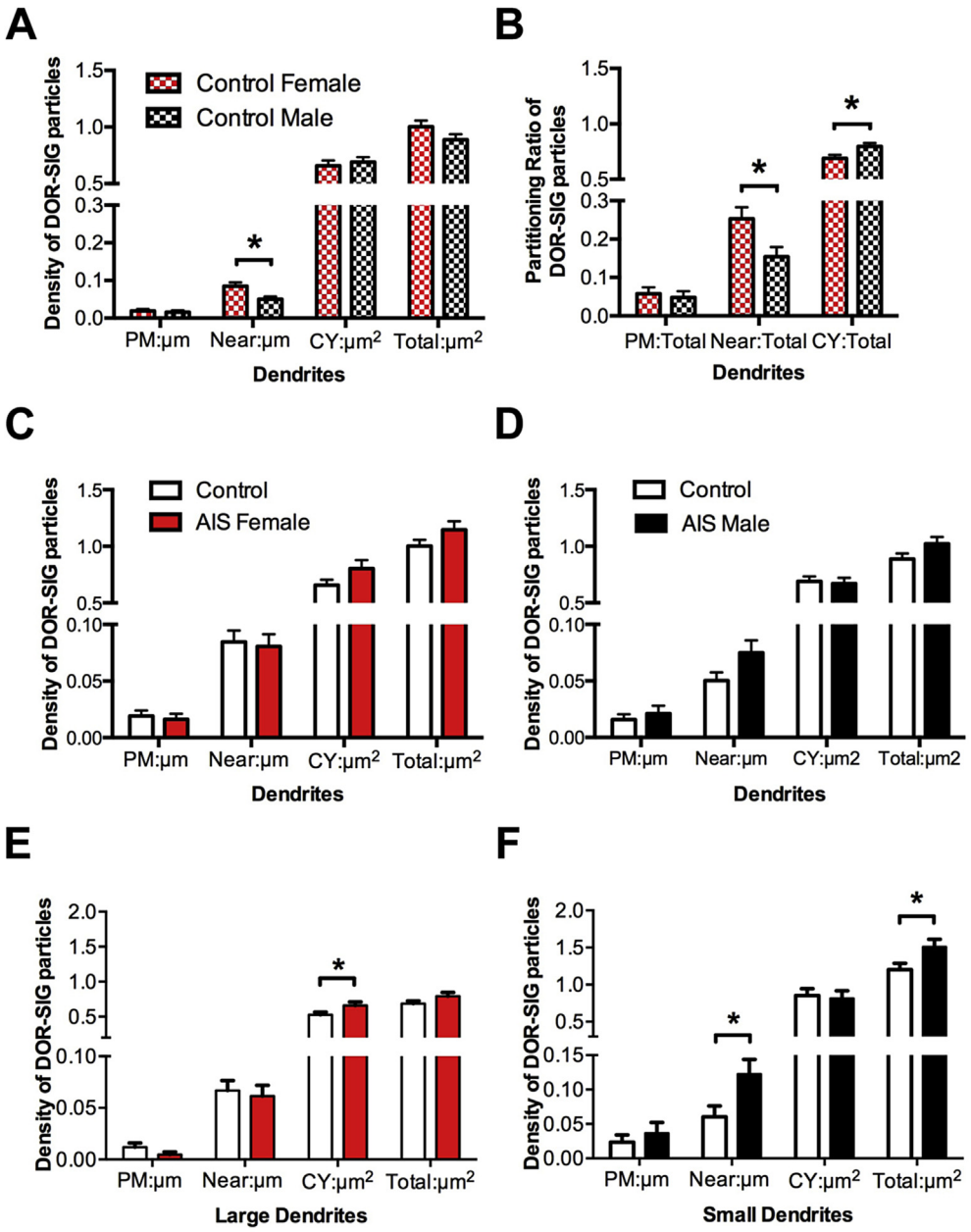

Fig. 3. Sex differences in the distribution of DOR-SIG particles in CA3 pyramidal cell dendrites at baseline and following AIS. **A**. In control rats, the density of near plasmalemmal DOR-SIG particles in dendrites in significantly greater (*$p < 0.05$) in proestrus females compared to males. **B**. Compared to males, the partitioning ratio of DOR-SIG particles in dendrites was significantly elevated near the plasmalemma (*$p < 0.05$) and significantly less in the cytoplasm (*$p < 0.05$). **C, D**. AIS did not significantly alter the density of DOR-SIG particles in any cellular compartment in dendrites in either proestrus females or males. **E**. After AIS, there was a significant increase (*$p < 0.05$) in cytoplasmic density of DOR-SIG particles in large dendrites of proestrus females. **F**. After AIS, there was a significant increase in the near plasmalemma and total densities (*$p < 0.05$) of DOR-SIG particles in small dendrites of males. N = 3 rats group; n = 50 dendrites per rat.

3.6. Acute oxycodone in CIS females redistributed DORs to the membrane of CA3 and hilar interneuron dendrites

The above results showed that females compared to males have higher baseline levels of near-plasmalemmal DORs in CA3 pyramidal cell dendrites (sec. 3.2) and a higher percentage of CA3 DOR-labeled spines contacted by mossy fibers (sec. 3.3). Following CIS in females, but not males, the density of near-plasmalemmal DOR-SIGs in CA3 pyramidal cell dendrites did not change and the density of near-plasmalemmal DOR-SIGs increased in hilar GABAergic dendrites. These results suggest that DORs in the female hippocampus, especially after CIS, are positioned to be activated by DOR agonist. Thus, to test this hypothesis, a subsequent experiment examined the acute affect of oxycodone on the redistribution of DOR-SIGs in a separate cohort of CIS females. In this experiment the distribution of DORs in either CA3 or dentate hilar interneurons of CIS estrus females was examined 1 h after an injection of the opioid agonist oxycodone (3 mg/kg, i.p.).

By light microscopy, acute oxycodone had no significant effect on the density of DOR-ir in stratum radiatum of CA3 and no significant effect on the number of DOR-labeled hilar interneurons (not shown). By EM, acute oxycodone did not alter the density or partitioning ratio of DOR-SIG particles in CA3 pyramidal cell dendrites in CIS females (not shown). However, the percentage of DOR-

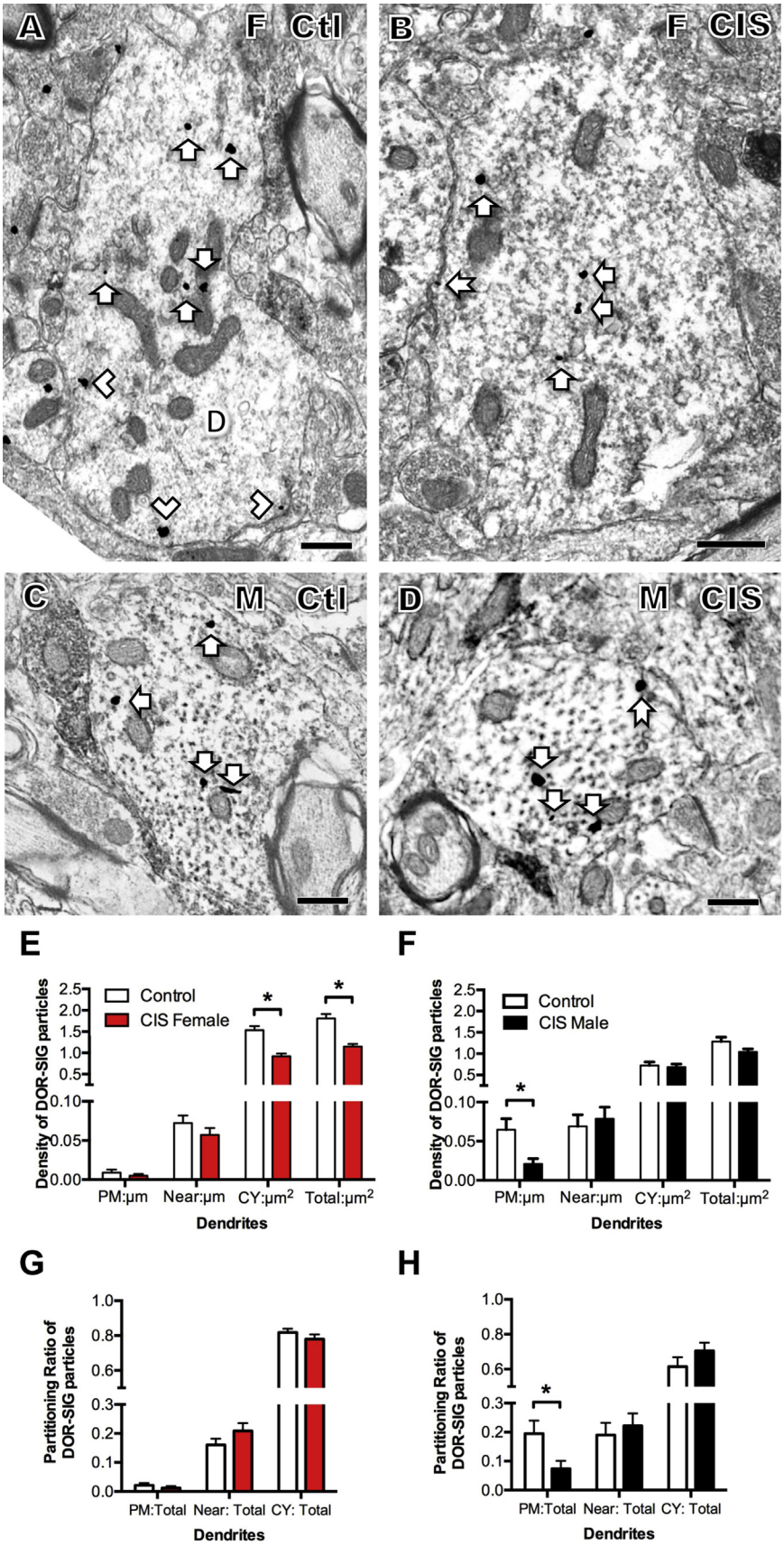

Fig. 4. Sex differences in the distribution of DOR-SIG particles in CA3 pyramidal cell dendrites following CIS. **A**–**D**. Representative electron micrographs show the distribution of DOR-SIG particles in dendrites from a control diestrus female (A) and control male (B) and CIS diestrus female (C) and CIS male (D). Examples of plasmalemmal (arrow with tail), near plasmalemmal (chevron) and cytoplasmic (arrow) DOR-SIG particles in dendrites are shown. After CIS, cytoplasmic DOR-SIG particles decrease in diestrus females. Scale bars A, B = 500 nm. **E**. After CIS, the cytoplasmic and total density of DOR-SIG particles significantly decrease (*$p < 0.05$) in dendrites in females. **F**. After CIS, the density of DOR-SIG particles on the plasma membrane of CA3 dendrites significantly decreases in males. **G**. In diestrus females, the partitioning ratio of DOR-SIG particles in any cellular compartment in dendrites is not significantly different following CIS. **H**. In males, the partitioning ratio of DOR-SIG particles on plasma membrane in CA3 dendrites significantly decreases (*$p < 0.05$) different following CIS. N = 3 rats group; n = 50 dendrites per rat.

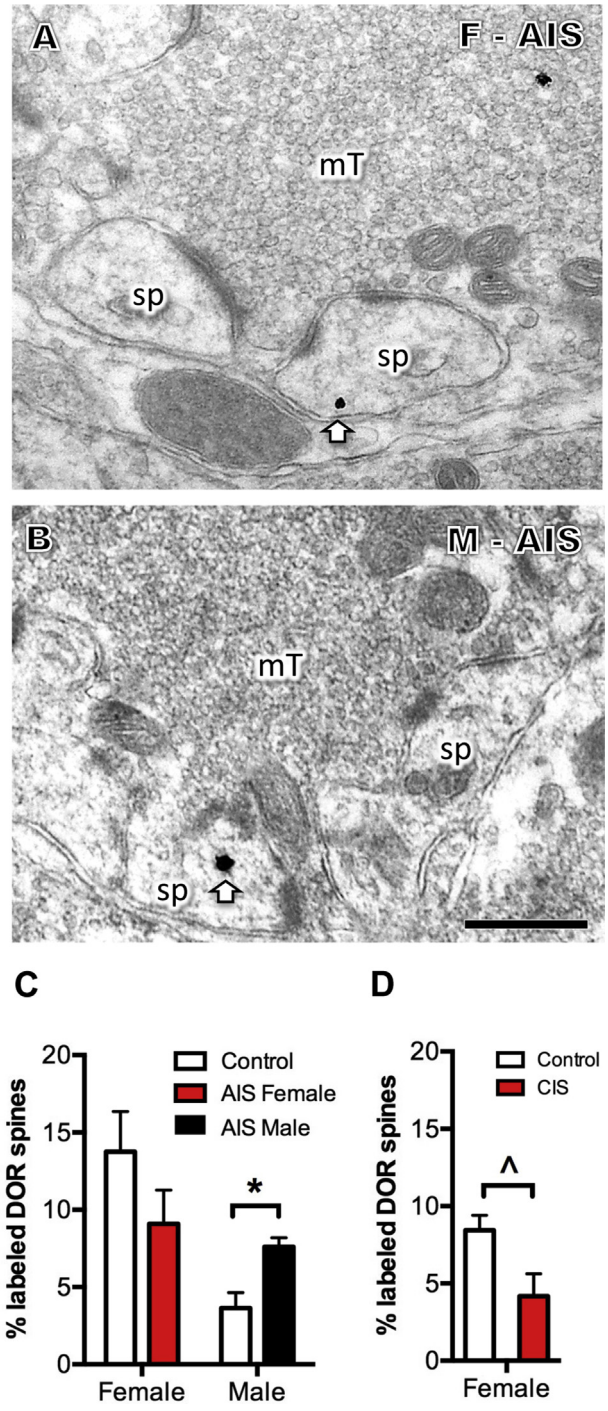

Fig. 5. Sex differences in the percentage of DOR-labeled dendritic spines that contact mossy fibers. A, B. Representative electron micrographs from an AIS proestrus female (A) and AIS male (B) show an example of a cytoplasmic DOR-SIG particle (arrow) in a dendritic spine (sp) contacted by a mossy fiber. Scale bar = 500 nm. **C.** After AIS, the percent of DOR-labeled spines contacted by mossy fibers significantly increases in males (*p < 0.05) but not proestrus females. **D.** After CIS, the percent DOR-labeled spines contacted by mossy fibers approaches a significant decrease (^p = 0.053) in diestrus females. N = 3 rats group; n = 50 mossy fibers per rat.

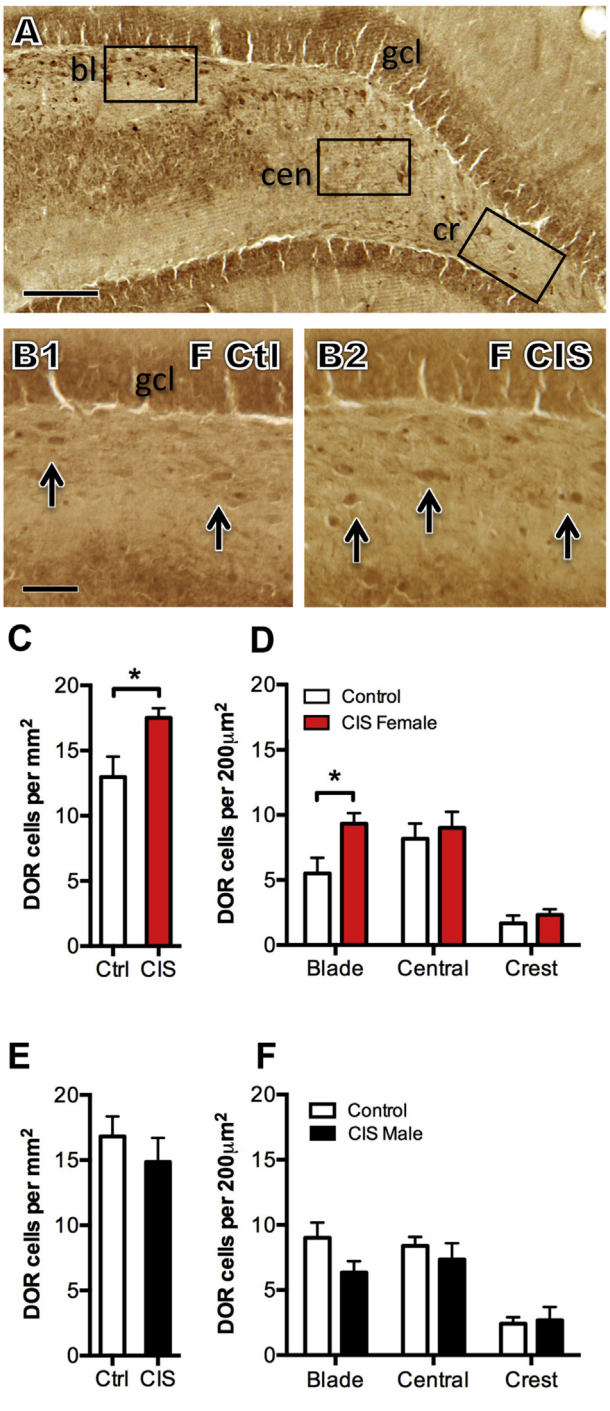

Fig. 6. Sex differences in the number of DOR labeled dentate hilar interneurons following CIS. A. Representative light micrograph from the dorsal dentate gyrus of a control female rat shows DOR-labeled neurons in the dorsal blade (bl), central (cen) and crest (cr) region of the hilus. **B1,2.** Representative micrographs of the dorsal blade from control and CIS diestrus females. Arrows indicate examples of DOR-labeled cells. gcl = granule cell layer Scale bar A = 200 µm; B = 100 µm. **C.** Following CIS, density of DOR-labeled cells in the hilus significantly increases in diestrus females (*p < 0.05). **D.** Analysis of the subregions of the hilus shows that after CIS the number of DOR-labeled cells significantly increases (*p < 0.05) selectively in the dorsal blade. **E.** In males, the density of DOR-labeled cells in the hilus did not significantly change following CIS. **F.** Following CIS, the numbers of DOR-labeled cells did not change in any hilar subregion in males. N = 5–6 rats per condition.

labeled spines contacted by mossy fibers following acute oxycodone administration approached a significant increase ($t_{2.86} = -3.11$, $p = 0.0564$; Fig. 9D). Moreover, EM analysis revealed that the partitioning ratio of the DOR-SIG particles significantly decreased in near the plasmalemma ($t_{146.3} = -3.10$, $P = 0.0023$) and significantly increased ($t_{239.3} = 3.02$, $p = 0.0028$) on the plasmalemma in the small dendrites (Fig. 9A–C).

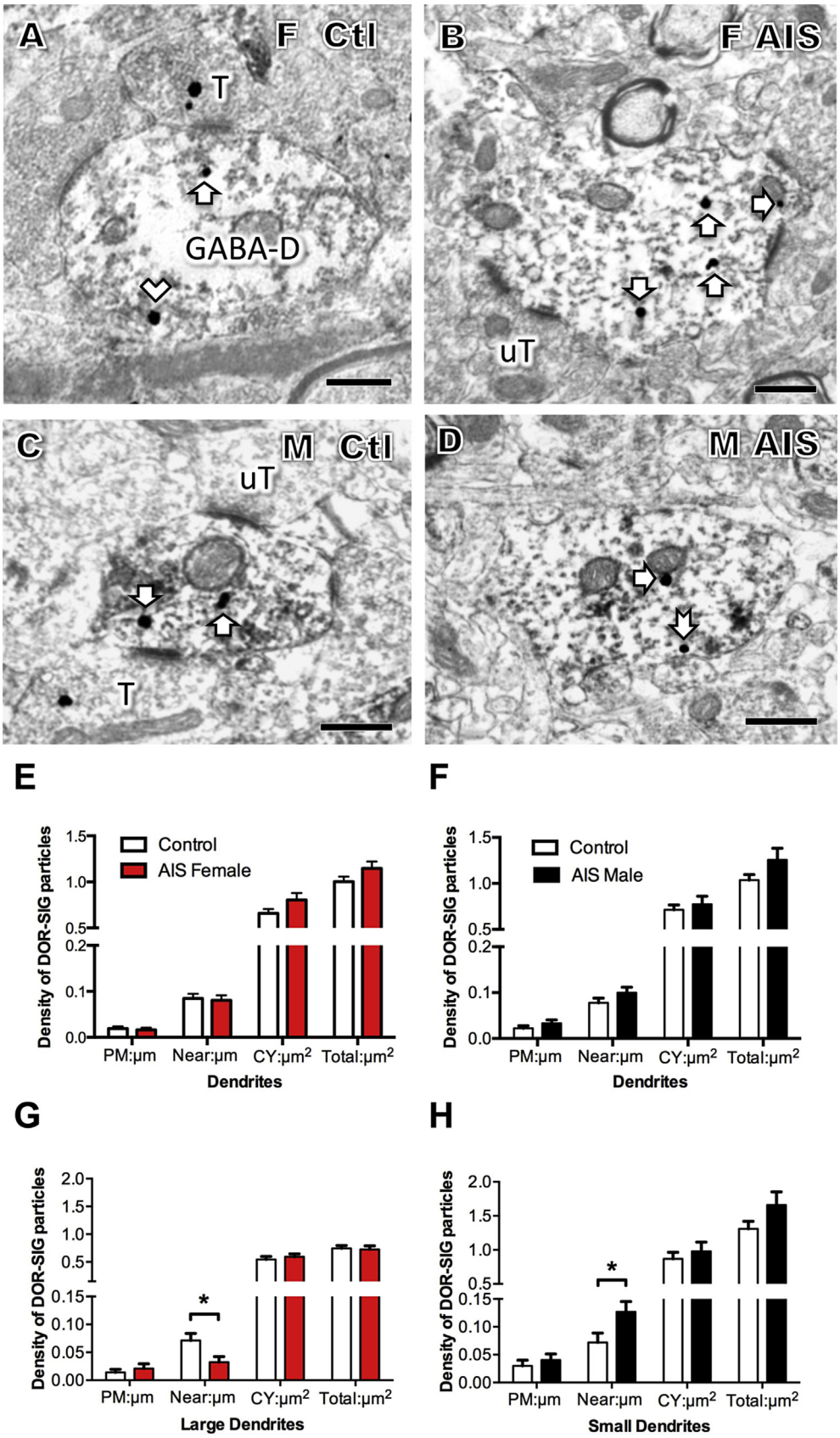

Fig. 7. Sex differences in the distribution of DOR-SIG particles in GABAergic hilar dendrites following AIS. **A**–**D**. Representative electron micrographs show the distribution of DOR-SIG particles in GABA-labeled dendrites (GABA-D) from a control proestrus female (A) and control male (B) and AIS proestrus female (C) and AIS male (D). Examples of plasmalemmal (arrow with tail), near plasmalemmal (chevron) and cytoplasmic (arrow) DOR-SIG particles in dendrites are shown. After AIS, the density of near plasmalemmal DOR-SIG particles increases in males. T = terminal; uT = unlabeled terminal. Scale bars A, B = 500 nm. **E, F.** AIS did not significantly alter the density of DOR-SIG particles in any cellular compartment in GABA-labeled dendrites in either proestrus females or males. **G.** After AIS, the density of DOR-SIG particles significantly decreased ($p < 0.05$) near the plasmalemma of large GABA-labeled dendrites in proestrus females. **H.** After AIS, the near plasmalemmal density of DOR-SIG particles significantly increased ($p < 0.05$) in small GABA-labeled dendrites in males.

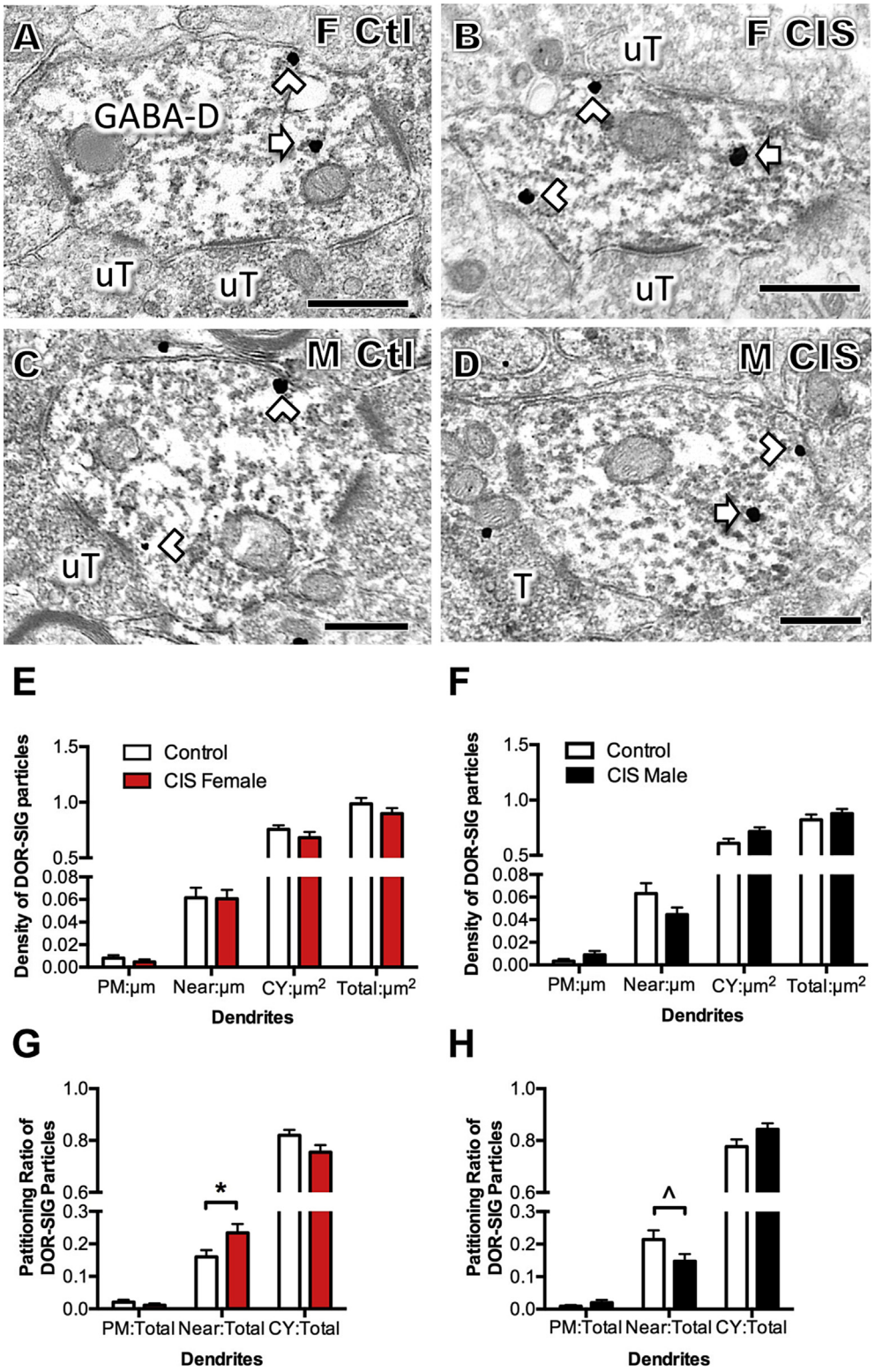

Fig. 8. Sex differences in the distribution of DOR-SIG particles in GABAergic hilar dendrites following CIS. A–D. Representative electron micrographs show the distribution of DOR-SIG particles in GABA-labeled dendrites (GABA-D) from a control diestrus female (A) and control male (B) and CIS diestrus female (C) and CIS male (D). Examples of near plasmalemmal (chevron) and cytoplasmic (arrow) DOR-SIG particles in dendrites are shown. After CIS, the partitioning ratio of near plasmalemmal DOR-SIG particles increases in females. T = terminal; uT = unlabeled terminal. Scale bars A, B = 500 nm. **E, F.** CIS did not significantly alter the density of DOR-SIG particles in any cellular compartment in GABA-labeled dendrites in either diestrus females or males. **G.** After CIS, the partitioning ratio of near plasmalemmal DOR-SIG particles in GABA-labeled dendrites significantly increases ($^{*}p < 0.05$) in diestrus females. **H.** There is an approaching significant decrease ($^{\wedge}p = 0.06$) in partitioning ratio of near plasmalemma DOR-SIG particles in GABA-labeled dendrites in males. N = 3 rats group; n = 50 dendrites per rat.

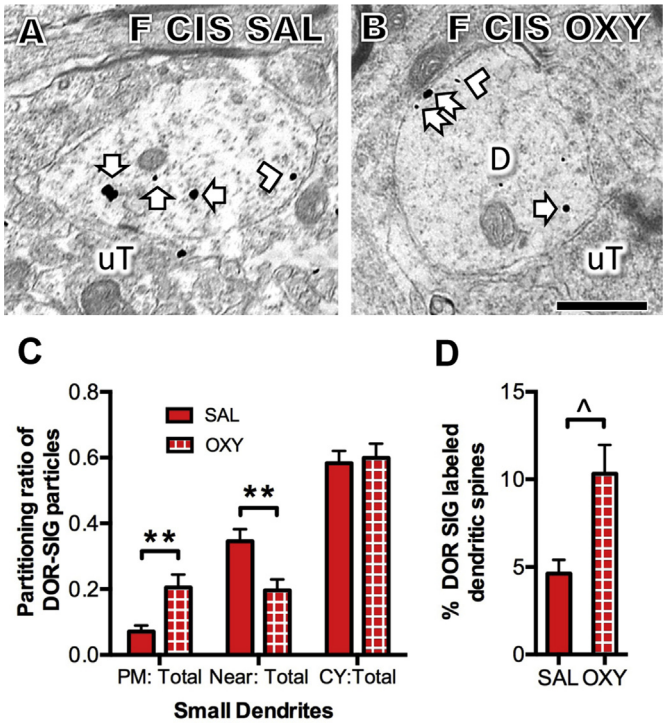

Fig. 9. Effect of acute oxycodone on the distribution of DOR-SIG particles in CA3 and dentate hilar dendrites in CIS females. A, B. Representative electron micrographs show the distribution of DOR-SIG particles in hilar dendrites from a saline and oxycodone injected CIS estrus females. Examples of plasmalemmal (arrow with tail), near plasmalemmal (chevron) and cytoplasmic (arrow) DOR-SIG particles in dendrites are shown. Scale bars A, B = 500 nm. **C.** One hour after oxycodone (3 mg/kg, I.P.), the partitioning ratio of DOR-SIG particles significantly increases on the plasmalemma and significantly decreases near the plasmalemma of hilar dendrites in CIS estrus females (**$p < 0.01$). **D.** One hour after oxycodone, the percent of DOR-labeled dendritic spines contacted by mossy fibers approaches a significant increase (^$p = 0.056$). N = 3 rats per group; n = 50 dendrites (C) or mossy fibers (D) per rat.

4. Discussion

These studies demonstrate that acute and chronic stress alter the levels and trafficking of DORs in hippocampal neurons both female and male rats. In particular, electron microscopic studies reveal that DORs redistribute within CA3 pyramidal cells and dentate hilar GABAergic interneurons in a sexually dimorphic manner that would promote activation and LTP in males after AIS and in females after CIS (Fig. 10). This redistribution of DORs is consistent with known sex differences in learning and memory tasks after stress: males display better cognitive performance after acute stress whereas females display better cognitive performance after chronic stress (Conrad et al., 2003; Kitraki et al., 2004; Luine et al., 2007). Thus, these results suggest that acute and chronic stress could affect opioid-related learning differentially in males and females.

4.1. Baseline sex differences in the distribution of DORs in hippocampal neurons

Our studies showed baseline sex differences in the levels and distribution of DORs in CA3 pyramidal cells, but not granule cells, which depended upon hormonal state of the females. The sex difference in the redistribution of DORs in CA3 pyramidal cell dendrites is similar to that observed previously in CA1 pyramidal cell dendrites (Williams et al., 2011b). By light microscopy, the levels of DORs were decreased in CA3 pyramidal cell dendritic fields in proestrus (high estrogen levels) compared to diestrus (low estrogen levels) whereas the DOR levels in males was closer to that seen in diestrus females. By electron microscopy, CA3 pyramidal cell dendrites in proestrus females compared to males had fewer near plasmalemmal DORs and greater DOR-labeled spines contacted by mossy fibers. This redistribution of DORs is thought to mediate the low-frequency mediated LTP in mossy fiber-CA3 synapses that is seen in proestrus females but not diestrus females or males (Harte-Hargrove et al., 2015) (Fig. 10).

Several lines of evidence support the possibility that signaling mechanisms for DOR and CRF receptors could interact in CA3 pyramidal cells and that sex and/or hormone levels could influence this interaction in response to stress. In addition to DORs, CA3 pyramidal cell dendrites contain CRF receptors (H. McAlinn, T.A. Milner unpublished data). Our previous studies in CA1 have shown that proestrus females compared to males have higher numbers of pyramidal cell dendrites that colabel for DOR and CRF1 with a greater proportion of CRF1 on the plasma membrane (Williams et al., 2011a). Further, the DOR agonist SNC80 can inhibit CRF mediated cyclic AMP accumulation in hormone sensitive NG108-15 cells (Williams et al., 2011a). Ligand activation of either DOR or CRF receptor relies upon the presentation of these receptors to the plasma membrane (Bangasser et al., 2010; Pradhan et al., 2009). The balance of the signaling cascades activated by DOR or CRF receptor may depend upon which receptor predominates on the plasma membrane at the time of the stressor. In the case of drug naïve, unstressed rats this balance could be altered following both acute and chronic stress.

4.2. Sex differences in DOR redistribution after AIS

Although our light microscopic studies showed that AIS resulted in decreased levels of DOR-labeling in the stratum radiatum of CA3 in both females and males, our electron microscopic studies revealed that AIS had different effects on the subcellular distribution of DORs within CA3 pyramidal cell dendrites. Specifically, after AIS the density of DORs was increased in the cytoplasmic compartment of large dendrites in females and increased in the near-plasmalemmal compartment of small dendrites in males. Additionally, AIS significantly increased the percentage of DOR labeled dendritic spines contacted by mossy fibers in males, but not females. This sexually dimorphic redistribution of DORs following AIS could have different functional consequences. In particular, although our findings suggest that the percent of DORs in CA3 dendritic spines remains high in females after AIS, the increase in the number of cytoplasmic DORs suggests more DORs being degraded or recycled (Fernandez-Monreal et al., 2012; Pierce et al., 2009). In contrast, our results suggest that following AIS, DORs are repositioned in the CA3 pyramidal cell dendrites of males where they would be more available for opioid ligand binding (Fig. 10). The increase in the percentage of DOR-labeled dendritic spines contacted by mossy fibers could affect the threshold for low frequency opioid-dependent LTP previously observed in proestrus females but not males (Harte-Hargrove et al., 2015). Moreover, as small dendrites generally receive a higher number of excitatory-type inputs (Froemke et al., 2005; Lovett-Barron et al., 2014), the AIS-induced increase in the pool of DORs ready to be inserted into the plasma membrane of distal CA3 dendrites could alter synaptic plasticity of these neurons following exposure to an opioid ligand or in response to release of opioids from entorhinal afferents (Fredens et al., 1984).

Following AIS, the subcellular redistribution of DORs in hilar GABAergic interneurons also differed between the sexes. Similar to CA3 pyramidal cell dendrites, AIS resulted in an increase of the near plasmalemmal DORs in small GABA-labeled dendrites in males. Moreover, in contrast to males, AIS resulted in a decrease in the

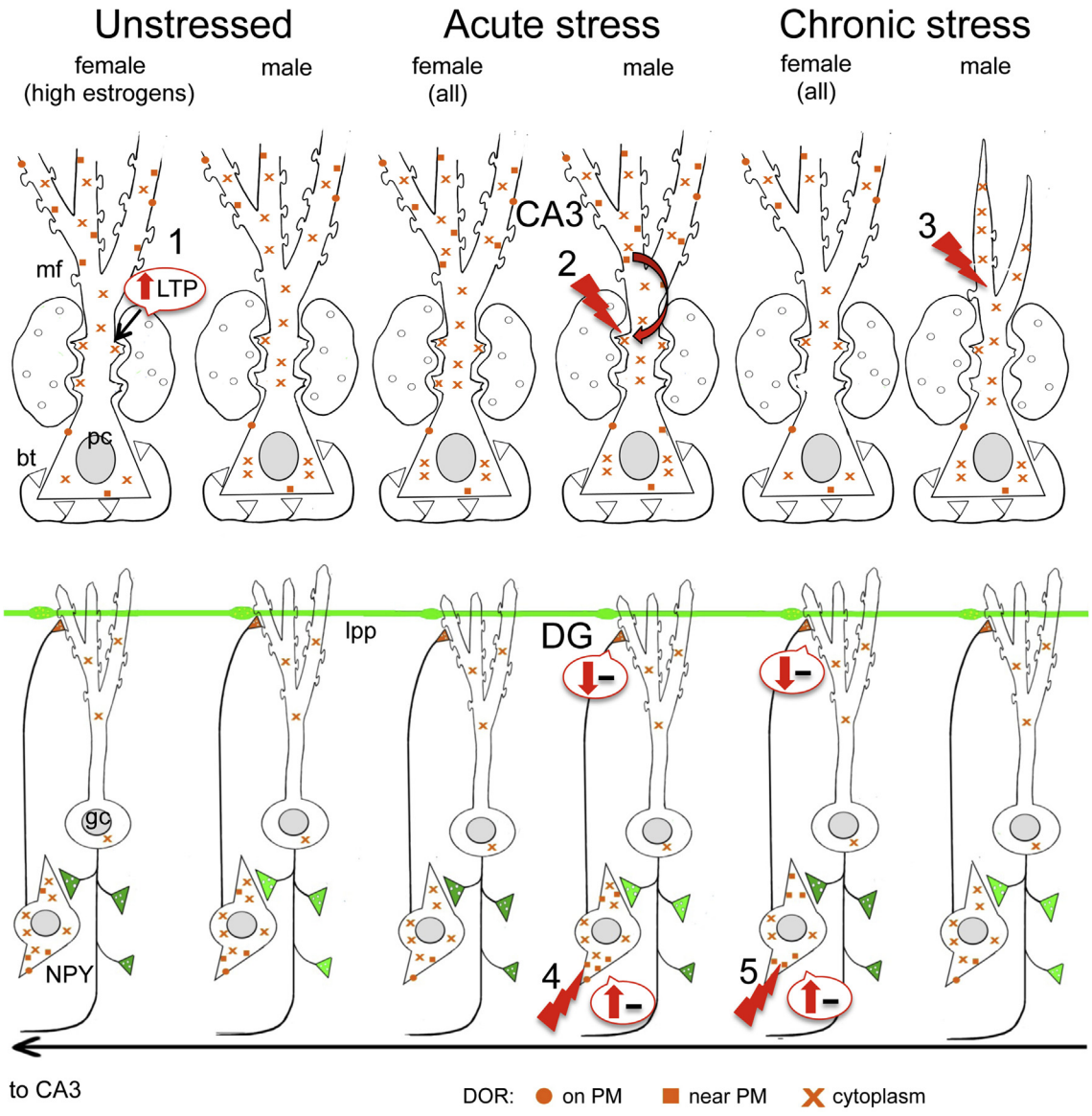

Fig. 10. Schematic shows sex differences in the hippocampal opioid system in unstressed, acute and chronic stressed rats. Arrows indicate predicted effects of DOR trafficking changes on inhibition (minus signs) in the CA3 and dentate gyrus (DG). # 1–5 indicate points where there are sex differences in the DOR distribution in unstressed rats and after AIS and CIS. Bt = basket cell terminals; mf = mossy fiber terminals; plasma membrane = PM. Green color indicates enkephalin levels. (For interpretation of the references to colour in this figure legend, the reader is referred to the web version of this article.)

(**1**) In unstressed conditions, DORs are increased in CA3 pyramidal cell dendritic spines (Harte-Hargrove et al., 2015) and decreased near the plasmalemma of the shafts of CA3 dendrites in high estrogen (proestrus) females compared to males. Moreover, low frequency (1 Hz) stimulation of the granule cells elicits a DOR-dependent LTP in CA3 of proestrus females that is not seen in diestrus females or males (Harte-Hargrove et al., 2015).
(**2**) After AIS, DORs decrease in the cytoplasm of CA3 dendritic shafts in females but increase in the near plasmalemma compartment of dendritic shafts and spines contacted by mossy fibers of CA3 pyramidal cells in males;
(**3**) After CIS, DORs decrease in the cytoplasm of dendritic shafts and spines contacted by mossy fibers in CA3 pyramidal cells in females and decrease near the plasma membrane of CA3 neuron dendritic shafts in males. Males, but not females, display an atrophy of CA3 pyramidal cell dendrites following (McEwen, 1999).
(**4**) Previous studies have shown that DORs are primarily in GABAergic dendrites containing NPY/SOM (Commons and Milner, 1996a; Williams and Milner, 2011; Williams et al., 2011b). GABAergic NPY/SOM interneurons are known to project to granule cell dendrites where they converge with entorhinal afferents from the lateral perforant path (lpp) (Sperk et al., 2007). After AIS, DORs in GABAergic interneuron dendrites decrease near the plasma membrane in females but increase near the plasmalemma in males.
(**5**) After CIS, DORs in GABAergic interneuron dendrites increase near the plasma membrane in females but decrease near the plasmalemma in males. The number of NPY-containing neurons decreased in CIS males but not CIS females (not shown).

near plasmalemmal DORs in large (proximal) GABA-labeled dendrites in females. In the rat hilus, large portions of the GABAergic interneurons contain NPY and SOM (Commons and Milner, 1996a; Williams and Milner, 2011; Williams et al., 2011b). GABAergic NPY/SOM interneurons are known to project to granule cell dendrites where they converge with entorhinal afferents (Sperk et al., 2007), many of which contain enkephalins (Commons and Milner, 1995). Together with the CA3 results, these findings suggest that following AIS in males alterations in the redistribution of DORs could especially impact the network properties of the opioid-containing entorhinal afferents in the hippocampus. In support of this assertion, a prominent role for DORs in entorhinal afferents to

the mouse CA1 region also has been reported (Rezai et al., 2013).

4.3. Sex differences in the expression of DOR in hilar interneurons after CIS

The expression of DOR immunoreactivity in hilar interneurons was elevated in females, but not males, following CIS. Further analysis revealed that this increase was limited to the dorsal blade region of the hilus. Our previous studies have shown that interneurons in the dorsal blade also contain high levels of phosphorylated DOR (Burstein et al., 2013) and phosphorylated MORs (pMOR) (Gonzales et al., 2011). Further, our previous studies also demonstrated the expression of pMOR labeling interneurons in the dorsal blade decreases in proestrus females and increases in males (Gonzales et al., 2011). Moreover, we also have shown that DOR and CRF colocalize to a similar extent in hilar interneurons in female and male rats (Williams and Milner, 2011). Thus, although chronic stress may activate DOR-containing interneurons in the hilus equally in both sexes, these findings suggest different signaling mechanisms may be recruited, resulting in opposite effects on the expression of opioid receptors.

The limitation of CIS related changes to the expression of DOR neurons to the dorsal blade of the dorsal dentate gyrus is interesting given the known anatomical and connectional differences from the ventral blade (for review see (Schmidt et al., 2012)) and the involvement of the opioid system in these differences. In particular, granule cells, which contain opioid peptides (Drake et al., 2007) in the dorsal blade develop earlier (Frotscher et al., 2007) and have greater dendritic lengths and spine densities (Claiborne et al., 1990; Desmond and Levy, 1985). Moreover, the ratio of granule cells to basket cells, which contain MORs (Milner et al., 2013), is about twice that seen in the ventral blade (95) and afferent projections from both the lateral entorhinal cortex (enkephalin containing (Drake et al., 2007)) and supramammilary nucleus (kappa opioid receptor containing (Drake et al., 1997)) are greater in the dorsal blade (Tamamaki and Nojyo, 1993). As to how sex differences in the redistribution of DORs play into these circuits following chronic stress is a topic for future investigations.

4.4. Sex differences in DOR redistribution after CIS

Like AIS, CIS also differentially altered the redistribution of DORs in hippocampal CA3 pyramidal cells and hilar interneurons in females and males (Fig. 10). Importantly, the pattern of the redistribution following CIS in both sexes was the opposite of that observed following AIS. Following CIS, cytoplasmic DORs decreased in the CA3 pyramidal cells in females whereas plasmalemmal DORs decrease in CA3 pyramidal cells in males. Additionally, the percentage of DOR-labeled dendritic spines contacted by mossy fibers in females was reduced following CIS. As the percentage of DOR-labeled spines correlates with the detection of low frequency opioid-dependent LTP in females and males (Harte-Hargrove et al., 2015), these results suggest the responses of CA3 pyramidal cells to opioids following CIS may be suboptimal in females. However, since the females examined in the CIS portion of the study were in diestrus, it is possible that the low estrogen levels contributed to this decrease in DOR-labeled spines (Williams et al., 2011b). Importantly, our studies showed that acute administration of oxycodone doubled the percentage of DOR-labeled spines contacted by mossy fibers.

CIS increased DORs in the near plasmalemmal compartment of hilar GABAergic dendrites in females but decreased DORs in the near plasmalemmal compartment of GABAergic dendrites in males (Fig. 10). This sexual dimorphism in the rearrangement of DORs could have significant functional consequences. As with the males following AIS, this suggests that CIS in females has increased the pool of DORs available for insertion into the plasma membrane of GABAergic (mostly NPY/SOM containing) interneurons following ligand exposure. Indeed our subsequent experiment demonstrated that one-hour after acute administration of oxycodone DORs moved from the near plasmalemmal compartment to the plasmalemmal compartment of GABA-labeled dendrites. Previous studies in mice demonstrate that DOR presentation to the plasma membrane of GABAergic interneurons is important for opioid-paired context learning (Faget et al., 2012). Thus, CIS in females, but not males, could prime females for enhanced context learning in response to opioids.

4.5. Functional considerations

Together with our previous studies, the present study reveals notable sex differences in the hippocampal opioid system and that acute and chronic stress have opposing affects on this system in females and males (Fig. 10). These changes are consistent with known sex differences in learning and memory tasks after stress: females display impaired cognitive performance after acute stress whereas males display impaired cognitive performance after chronic stress (Conrad et al., 2003; Kitraki et al., 2004; Luine et al., 2007; Weiss et al., 2005).

In unstressed female rats with high estrogen states compared to males, opioids and opioid receptors are arranged in a manner that enhances excitation and promotes learning processes. In females at high estrogen states compared to males, enkephalins levels are about two times higher and DORs are about three times greater in CA3 dendritic spines contacted by mossy fibers (Harte-Hargrove et al., 2015) and about twice as high near the plasma membrane of CA3 pyramidal cell dendrites. Additionally, females in high estrogen states compared to females in low estrogen states have more MORs on the plasma membrane of hilar GABA interneurons (Torres-Reveron et al., 2009). Moreover, females in high estrogen states, but not males, show a strong MOR regulation of mossy fiber transmission and a novel DOR-dependent form of mossy fiber-CA3 LTP (Harte-Hargrove et al., 2015).

In females, regardless of estrous state, acute stress decreases enkephalin levels (Pierce et al., 2014) and DORs and MORs traffic within CA3 pyramidal cells and GABA interneurons in a manner that would reduce excitation and learning processes. In contrast, acute stress has opposite and more limited effects on the opioid system in males: enkephalins are unchanged (Pierce et al., 2014), total MORs on PARV hilar neurons are slightly increased (Milner et al., 2013) and DORs are prepositioned in a manner that could promote mossy fiber-CA3 LTP and GABAergic disinhibition.

Our results suggest that chronic stress “primes” the opioid system in all females, regardless of estrous stage, in a manner that would promote excitation and learning processes following subsequent exposure either to stress or an opioid ligand. The opioid system in all females after CIS resembles that of females in elevated estrogen states: (1) the pool of available enkephalin is elevated in mossy fibers (Pierce et al., 2014); (2) DORs are decreased in the dendritic shafts in CA3 pyramidal cells; and (3) MORs are increased in the dendrites and terminals of PARV GABAergic interneurons in the dentate gyrus (Milner et al., 2013). Moreover, (4) after CIS in females, DORs have mobilized to the near-plasmalemma of the dendrites of GABAergic NPY/SOM interneurons known to project to granule cell dendrites where they converge with entorhinal afferents (Milner and Bacon, 1989; Milner and Veznedaroglu, 1992). Following acute oxycodone exposure, the DORs redistribute to the plasma membrane of dendrites in hilar GABAergic interneurons in CIS females. These findings suggest that a second mechanism for enhancing hippocampal excitation and perhaps drug-related

learning processes comes into play in females after CIS. Specifically, since DORs inhibit NPY release, activation of DORs on NPY-containing GABA interneurons could promote lateral perforant pathway LTP (Sperk et al., 2007).

Environmental context is an important component of drug acquisition and relapse (Crombag et al., 2008; Koob and Volkow, 2010) and sexual dimorphism in response to stress is important in these processes (Bangasser and Shors, 2010; Beck and Luine, 2010; Becker and Koob, 2016). Accumulating evidence indicates that connections between the dentate gyrus and CA3 region in the dorsal hippocampus are engaged in pattern separation, which includes learning that two events are the same despite variation (reviewed in (Schmidt et al., 2012)). Moreover, the finding that naloxone disrupts visual-spatial pattern completion in CA3b (Kesner and Warthen, 2010) indicates that opioids are involved. Thus, the current study, together with our previous studies, suggests that sexual dimorphism in the opioid system, especially in response to stress, would affect drug-related learning.

Conflict of interest

The authors declare no competing financial interests.

Acknowledgements

Study design: BSM, EMW, TAM; Data collection: SM, BSH, SO, KS, ADG, TVK, JS, TAM; Writing of report: SM, BSH, SO, BSM, EMW, TAM; Decision to submit for publication: SM, BSM, EMW, TAM. Supported by: NIH grants DA08259, HL098351, HL096571 (TAM), AG016765 (BSM, TAM), AG059850 (EMW) and T32 DA007274 (TAVK). We thank Ms. Mariana Dodos for assistance with the statistics and figures.

Appendix A. Supplementary data

Supplementary data related to this article can be found at http://dx.doi.org/10.1016/j.ynstr.2016.11.002.

References

Amaral, D.G., Dent, J.A., 1981. Development of the mossy fibers of the dentate gyrus. I. A light and electron microscopic study of the mossy fibers and their expansions. J. Comp. Neurol. 196, 51–86.
Bangasser, D.A., Curtis, A., Reyes, B.A., Bethea, T.T., Parastatidis, I., Ischiropoulos, H., Van Bockstaele, E.J., Valentino, R.J., 2010. Sex differences in corticotropin-releasing factor receptor signaling and trafficking: potential role in female vulnerability to stress-related psychopathology. Mol. Psychiatry. 15, 877, 896–877, 904.
Bangasser, D.A., Shors, T.J., 2010. Critical brain circuits at the intersection between stress and learning. Neurosci. Biobehav. Rev. 34, 1223–1233.
Bao, G., Kang, L., Li, H., Li, Y., Pu, L., Xia, P., Ma, L., Pei, G., 2007. Morphine and heroin differentially modulate in vivo hippocampal LTP in opiate-dependent rat. Neuropsychopharmacology. 32, 1738–1749.
Barg, J., Levy, R., Simantov, R., 1984. Up-regulation of opiate receptors by opiate antagonists in neuroblastoma-glioma cell culture: the possibility of interaction with guanosine triphosphate-binding proteins. Neurosci. Lett. 50, 133–137.
Beck, K.D., Luine, V.N., 2010. Evidence for sex-specific shifting of neural processes underlying learning and memory following stress. Physiol. Behav. 99, 204–211.
Becker, J.B., Hu, M., 2008. Sex differences in drug abuse. Front. Neuroendocrinol. 29, 36–47.
Becker, J.B., Koob, G.F., 2016. Sex differences in animal models: focus on addiction. Pharmacol. Rev. 68, 242–263.
Becker, J.B., Monteggia, L.M., Perrot-Sinal, T.S., Romeo, R.D., Taylor, J.R., Yehuda, R., Bale, T.L., 2007. Stress and disease: is being female a predisposing factor? J. Neurosci. 27, 11851–11855.
Berke, J.D., Hyman, S.E., 2000. Addiction, dopamine, and the molecular mechanisms of memory. Neuron 25, 515–532.
Bie, B., Zhang, Z., Cai, Y.Q., Zhu, W., Zhang, Y., Dai, J., Lowenstein, C.J., Weinman, E.J., Pan, Z.Z., 2010. Nerve growth factor-regulated emergence of functional delta-opioid receptors. J. Neurosci. 30, 5617–5628.
Boudin, H., Pélaprat, D., Rostène, W., Pickel, V.M., Beaudet, A., 1998. Correlative ultrastructural distribution of neurotensin receptor proteins and binding sites in the rat substantia nigra. J. Neurosci. 18, 8473–8484.
Bruchas, M.R., Xu, M., Chavkin, C., 2008. Repeated swim stress induces kappa opioid-mediated activation of extracellular signal-regulated kinase 1/2. Neuroreport. 19, 1417–1422.
Burstein, S.R., Williams, T.J., Lane, D.A., Knudsen, M.G., Pickel, V.M., McEwen, B.S., Waters, E.M., Milner, T.A., 2013. The influences of reproductive status and acute stress on the levels of phosphorylated delta opioid receptor immunoreactivity in rat hippocampus. Brain Res. 1518, 71–81.
Claiborne, B.J., Amaral, D.G., Cowan, W.M., 1990. Quantitative, three-dimensional analysis of granule cell dendrites in th rat dentate gyrus. J. Comp. Neurol. 302, 206–219.
Commons, K.G., Milner, T.A., 1995. Ultrastructural heterogeneity of enkephalin-containing neurons in the rat hippocampal formation. J. Comp. Neurol. 358, 324–342.
Commons, K.G., Milner, T.A., 1996a. Cellular and subcellular localization of delta opiate receptor immunoreactivity in the rat dentate gyrus. Brain Res. 738, 181–195.
Commons, K.G., Milner, T.A., 1996b. The ultrastructural relationships between leu-enkephalin and GABA containing neurons differ within the hippocampal formation. Brain Res. 724, 1–15.
Commons, K.G., Milner, T.A., 1997. Localization of delta opiate receptor immunoreactivity in interneurons and pyramidal cells in the rat hippocampus. J. Comp. Neurol. 381, 373–387.
Conrad, C.D., Grote, K.A., Hobbs, R.J., Ferayorni, A., 2003. Sex differences in spatial and non-spatial Y-maze performance after chronic stress. Neurobiol. Learn. Mem. 79, 32–40.
Crain, B.J., Chang, K.J., McNamara, J.O., 1986. Quantitative autoradiographic analysis of mu and delta opioid binding sites in the rat hippocampal formation. J. Comp. Neurol. 246, 170–180.
Crombag, H.S., Bossert, J.M., Koya, E., Shaham, Y., 2008. Review. Context-induced relapse to drug seeking: a review. Philos. Trans. R. Soc. Lond B Biol. Sci. 363, 3233–3243.
Derrick, B.E., Rodriguez, S.B., Lieberman, D.N., Martinez Jr., J.L., 1992. Mu opioid receptors are associated with the induction of hippocampal mossy fiber long-term potentiation. J. Pharmacol. Exp. Ther. 263, 725–733.
Desmond, N.L., Levy, W.B., 1985. Granule cell dendritic spine density in the rat hippocampus varies with spine shape and location. Neurosci. Lett. 54, 219–224.
Drake, C.T., Chavkin, C., Milner, T.A., 1997. Kappa opioid receptor-like immunoreactivity is present in substance P-containing subcortical afferents in Guinea pig dentate gyrus. Hippocampus 7, 36–47.
Drake, C.T., Chavkin, C., Milner, T.A., 2007. Opioid systems in the dentate gyrus. Prog. Brain Res. 163, 245–814.
Elman, I., Karlsgodt, K.H., Gastfriend, D.R., 2001. Gender differences in cocaine craving among non-treatment-seeking individuals with cocaine dependence. Am. J. Drug Alcohol Abuse 27, 193–202.
Faget, L., Erbs, E., Le, M.J., Scherrer, G., Matifas, A., Benturquia, N., Noble, F., Decossas, M., Koch, M., Kessler, P., Vonesch, J.L., Schwab, Y., Kieffer, B.L., Massotte, D., 2012. In vivo visualization of delta opioid receptors upon physiological activation uncovers a distinct internalization profile. J. Neurosci. 32, 7301–7310.
Fernandez-Monreal, M., Brown, T.C., Royo, M., Esteban, J.A., 2012. The balance between receptor recycling and trafficking toward lysosomes determines synaptic strength during long-term depression. J. Neurosci. 32, 13200–13205.
Fiorentine, R., Anglin, M.D., Gil-Rivas, V., Taylor, E., 1997. Drug treatment: explaining the gender paradox. Subst. Use. Misuse. 32, 653–678.
Fredens, K., Stengaard Pedersen, K., Larsson, L.I., 1984. Localization of enkephalin and cholecystokinin immunoreactivities in the perforant path terminal fields of the rat hippocampal formation. Brain Res. 304, 255–263.
Froemke, R.C., Poo, M.M., Dan, Y., 2005. Spike-timing-dependent synaptic plasticity depends on dendritic location. Nature 434, 221–225.
Frotscher, M., Zhao, S., Forster, E., 2007. Development of cell and fiber layers in the dentate gyrus. Prog. Brain Res. 163, 133–142.
Gonzales, K.L., Chapleau, J.D., Pierce, J.P., Kelter, D.T., Williams, T.J., Torres-Reveron, A., McEwen, B.S., Waters, E.M., Milner, T.A., 2011. The influences of reproductive status and acute stress on the levels of phosphorylated mu opioid recetpor immunoreactivity in rat hippocampus. Front. Neuroendocrinol. 2, 1–10.
Gulya, K., Gehlert, D.R., Wamsley, J.K., Mosberg, H., Hruby, V.J., Yamamura, H.I., 1986. Light microscopic autoradiographic localization of delta opioid receptors in the rat brain using a highly selective bis-penicillamine cyclic enkephalin analog. J. Pharmacol. Exp. Ther. 238, 720–726.
Haberstock-Debic, H., Wein, M., Barrot, M., Colago, E.E., Rahman, Z., Neve, R.L., Pickel, V.M., Nestler, E.J., Von Zastrow, M., Svingos, A.L., 2003. Morphine acutely regulates opioid receptor trafficking selectively in dendrites of nucleus accumbens neurons. J. Neurosci. 23, 4324–4332.
Harte-Hargrove, L.C., Varga-Wesson, A., Duffy, A.M., Milner, T.A., Scharfman, H.E., 2015. Opioid receptor-dependent sex differences in synaptic plasticity in the hippocampal mossy fiber pathway of the adult rat. J. Neurosci. 35, 1723–1738.
Hu, M., Crombag, H.S., Robinson, T.E., Becker, J.B., 2004. Biological basis of sex differences in the propensity to self-administer cocaine. Neuropsychopharmacology 29, 81–85.
Hu, W., Zhang, M., Czeh, B., Flugge, G., Zhang, W., 2010. Stress impairs GABAergic network function in the hippocampus by activating nongenomic glucocorticoid receptors and affecting the integrity of the parvalbumin-expressing neuronal network. Neuropsychopharmacology 35, 1693–1707.

Kesner, R.P., Warthen, D.K., 2010. Implications of CA3 NMDA and opiate receptors for spatial pattern completion in rats. Hippocampus. 20, 550–557.
Kieffer, B.L., Befort, K., Gaveriaux-Ruff, C., Hirth, C.G., 1992. The delta opioid receptor: isolation of a cDNA by expression cloning and pharmacological characterization. Proc. Natl. Acad. Sci. U. S. A. 89, 12048–12052.
Kilts, C.D., Schweitzer, J.B., Quinn, C.K., Gross, R.E., Faber, T.L., Muhammad, F., Ely, T.D., Hoffman, J.M., Drexler, K.P., 2001. Neural activity related to drug craving in cocaine addiction. Arch. Gen. Psychiatry. 58, 334–341.
Kitraki, E., Kremmyda, O., Youlatos, D., Alexis, M.N., Kittas, C., 2004. Gender-dependent alterations in corticosteroid receptor status and spatial performance following 21 days of restraint stress. Neuroscience. 125, 47–55.
Koob, G.F., 2008. A role for brain stress systems in addiction. Neuron. 59, 11–34.
Koob, G.F., Volkow, N.D., 2010. Neurocircuitry of addiction. Neuropsychopharmacology 35, 217–238.
Lauder, J.M., Han, V.K.M., Henderson, P., Towle, A.C., 1986. Prenatal ontogeny of the GABAergic system in the rat brain: an immunocytochemical study. Neurosci. 19, 465–493.
Ledoux, V.A., Smejkalova, T., May, R.M., Cooke, B.M., Woolley, C.S., 2009. Estradiol facilitates the release of neuropeptide Y to suppress hippocampus-dependent seizures. J. Neurosci. 29, 1457–1468.
Lovett-Barron, M., Kaifosh, P., Kheirbek, M.A., Danielson, N., Zaremba, J.D., Reardon, T.R., Turi, G.F., Hen, R., Zemelman, B.V., Losonczy, A., 2014. Dendritic inhibition in the hippocampus supports fear learning. Science 343, 857–863.
Lucas, L.R., Wang, C.J., McCall, T.J., McEwen, B.S., 2007. Effects of immobilization stress on neurochemical markers in the motivational system of the male rat. Brain Res. 1155 (108–15), 108–115. Epub;%2007 Apr 27.
Luine, V.N., Beck, K.D., Bowman, R.E., Frankfurt, M., MacLusky, N.J., 2007. Chronic stress and neural function: accounting for sex and age. J. Neuroendocrinol. 19, 743–751.
Luo, A.H., Tahsili-Fahadan, P., Wise, R.A., Lupica, C.R., Aston-Jones, G., 2011. Linking context with reward: a functional circuit from hippocampal CA3 to ventral tegmental area. Science. 333, 353–357.
Lynch, W.J., Arizzi, M.N., Carroll, M.E., 2000. Effects of sex and the estrous cycle on regulation of intravenously self-administered cocaine in rats. Psychopharmacol. Berl. 152, 132–139.
Mansour, A., Fox, C.A., Burke, S., Meng, F., Thompson, R.C., Akil, H., Watson, S.J., 1994. Mu, delta, and kappa opioid receptor mRNA expression in the rat CNS: an in situ hybridization study. J. Comp. Neurol. 350, 412–438.
Mansour, A., Khachaturian, H., Lewis, M.E., Akil, H., Watson, S.J., 1987. Autoradiographic differentiation of mu, delta, and kappa opioid receptors in the rat forebrain and midbrain. J. Neurosci. 7, 2445–2464.
McEwen, B.S., 1999. Stress and hippocampal plasticity. Annu. Rev. Neurosci. 22, 105–122.
McEwen, B.S., Milner, T.A., 2017. Understanding the broad influence of sex hormones and sex differences in the brain. J. Neurosci. Res. 95, 24–39.
McLean, S., Rothman, R.B., Jacobson, A.E., Rice, K.C., Herkenham, M., 1987. Distribution of opiate receptor subtypes and enkephalin and dynorphin immunoreactivity in the hippocampus of squirrel, Guinea pig, rat, and hamster. J. Comp. Neurol. 255, 497–510.
Milner, T.A., Bacon, C.E., 1989. Ultrastructural localization of somatostatin-like immunoreactivity in the rat dentate gyrus. J. Comp. Neurol. 290, 544–560.
Milner, T.A., Burstein, S.R., Marrone, G.F., Khalid, S., Gonzalez, A.D., Williams, T.J., Schierberl, K.C., Torres-Reveron, A., Gonzales, K.L., McEwen, B.S., Waters, E.M., 2013. Stress differentially alters mu opioid receptor density and trafficking in parvalbumin-containing interneurons in the female and male rat hippocampus. Synapse 67, 757–772.
Milner, T.A., Veznedaroglu, E., 1992. Ultrastructural localization of neuropeptide Y-like immunoreactivity in the rat hippocampal formation. Hippocampus 2, 107–126.
Milner, T.A., Waters, E.M., Robinson, D.C., Pierce, J.P., 2011. Degenerating processes identified by electron microscopic immunocytochemical methods. In: Manfredi, G., Kawamata, H. (Eds.), Neurodegeneration, Methods and Protocols. Springer, New York, pp. 23–59.
Milner, T.A., Wiley, R.G., Kurucz, O.S., Prince, S.R., Pierce, J.P., 1997. Selective changes in hippocampal neuropeptide Y neurons following removal of the cholinergic septal inputs. J. Comp. Neurol. 386, 46–59.
Olive, M.F., Anton, B., Micevych, P., Evans, C.J., Maidment, N.T., 1997. Presynaptic versus postsynaptic localization of m and d opioid receptors in dorsal and ventral striatopallidal pathways. J. Neurosci. 17, 7471–7479.
Olmstead, M.C., Burns, L.H., 2005. Ultra-low-dose naltrexone suppresses rewarding effects of opiates and aversive effects of opiate withdrawal in rats. Psychopharmacol. Berl. 181, 576–581.
Persson, A.I., Thorlin, T., Eriksson, P.S., 2005. Comparison of immunoblotted delta opioid receptor proteins expressed in the adult rat brain and their regulation by growth hormone. Neurosci. Res. 52, 1–9.
Persson, P.A., Thorlin, T., Ronnback, L., Hansson, E., Eriksson, P.S., 2000. Differential expression of delta opioid receptors and mRNA in proliferating astrocytes during the cell cycle. J. Neurosci. Res. 61, 371–375.
Peters, A., Palay, S.L., Webster, H.d, 1991. The Fine Structure of the Nervous System, third ed. Oxford University Press, New York.
Pierce, J.P., Kelter, D.T., McEwen, B.S., Waters, E.M., Milner, T.A., 2014. Hippocampal mossy fiber leu-enkephalin immunoreactivity in female rats is significantly altered following both acute and chronic stress. J. Chem. Neuroanat. 55, 9–17.
Pierce, J.P., Kievits, J., Graustein, B., Speth, R.C., Iadecola, C., Milner, T.A., 2009. Sex differences in the subcellular distribution of angiotensin type 1 receptors and NADPH oxidase subunits in the dendrites of C1 neurons in the rat rostral ventrolateral medulla. Neuroscience. 163, 329–338.
Pierce, J.P., Kurucz, O., Milner, T.A., 1999. The morphometry of a peptidergic transmitter system before and after seizure. I. Dynorphin B-like immunoreactivity in the hippocampal mossy fiber system. Hippocampus 9, 255–276.
Pradhan, A.A., Becker, J.A., Scherrer, G., Tryoen-Toth, P., Filliol, D., Matifas, A., Massotte, D., Gaveriaux-Ruff, C., Kieffer, B.L., 2009. In vivo delta opioid receptor internalization controls behavioral effects of agonists. PLoS One. 4, e5425.
Rezai, X., Kieffer, B.L., Roux, M.J., Massotte, D., 2013. Delta opioid receptors regulate temporoammonic-activated feedforward inhibition to the mouse CA1 hippocampus. PLoS One. 8, e79081.
Risinger, F.O., Oakes, R.A., 1995. Nicotine-induced conditioned place preference and conditioned place aversion in mice. Pharmacol. Biochem. Behav. 51, 457–461.
Robbins, S.J., Ehrman, R.N., Childress, A.R., O'Brien, C.P., 1999. Comparing levels of cocaine cue reactivity in male and female outpatients. Drug Alcohol Depend. 53, 223–230.
Rogers, S.A., Kempen, T.A., Pickel, V.M., Milner, T.A., 2016. Enkephalin levels and the number of neuropeptide Y-containing interneurons in the hippocampus are decreased in female cannabinoid-receptor 1 knock-out mice. Neurosci. Lett. 620, 97–103.
Saland, L.C., Hastings, C.M., Abeyta, A., Chavez, J.B., 2005. Chronic ethanol modulates delta and mu-opioid receptor expression in rat CNS: immunohistochemical analysis with quantitiative confocal microscopy. Neurosci. Lett. 381, 163–168.
Scherrer, G., Imamachi, N., Cao, Y.Q., Contet, C., Mennicken, F., O'Donnell, D., Kieffer, B.L., Basbaum, A.I., 2009. Dissociation of the opioid receptor mechanisms that control mechanical and heat pain. Cell 137, 1148–1159.
Schmidt, B., Marrone, D.F., Markus, E.J., 2012. Disambiguating the similar: the dentate gyrus and pattern separation. Behav. Brain Res. 226, 56–65.
Shalev, U., Highfield, D., Yap, J., Shaham, Y., 2000. Stress and relapse to drug seeking in rats: studies on the generality of the effect. Psychopharmacol. Berl. 150, 337–346.
Shansky, R.M., Hamo, C., Hof, P.R., Lou, W., McEwen, B.S., Morrison, J.H., 2010. Estrogen promotes stress sensitivity in a prefrontal cortex-amygdala pathway. Cereb. Cortex. 20, 2560–2567.
Sperk, G., Hamilton, T., Colmers, W.F., 2007. Neuropeptide Y in the dentate gyrus. Prog. Brain Res. 163, 285–297.
Swanson, L.W., 1992. Brain Maps: Structure of the Rat Brain, 1 edn. Elsevier, Amsterdam.
Tamamaki, N., Nojyo, Y., 1993. Projection of the entorhinal layer II neurons in the rat as revealed by intracellular pressure-injection of neurobiotin. Hippocampus 3, 471–480.
Torres-Reveron, A., Khalid, S., Williams, T.J., Waters, E.M., Drake, C.T., McEwen, B.S., Milner, T.A., 2008. Ovarian steroids modulate leu-enkephalin levels and target leu-enkephalinergic profiles in the female hippocampal mossy fiber pathway. Brain Res. 1232 (70–84), 70–84.
Torres-Reveron, A., Williams, T.J., Chapleau, J.D., Waters, E.M., McEwen, B.S., Drake, C.T., Milner, T.A., 2009. Ovarian steroids alter mu opioid receptor trafficking in hippocampal parvalbumin GABAergic interneurons. Exp. Neurol. 219, 319–327.
Turner, C.D., Bagnara, J.T., 1971. General Endocrinology. W.B. Saunders, Philadelphia.
Volkow, N.D., Wang, G.J., Telang, F., Fowler, J.S., Logan, J., Childress, A.R., Jayne, M., Ma, Y., Wong, C., 2006. Cocaine cues and dopamine in dorsal striatum: mechanism of craving in cocaine addiction. J. Neurosci. 26, 6583–6588.
Vorel, S.R., Liu, X., Hayes, R.J., Spector, J.A., Gardner, E.L., 2001. Relapse to cocaine-seeking after hippocampal theta burst stimulation. Science 292, 1175–1178.
Vyas, A., Mitra, R., Shankaranarayana Rao, B.S., Chattarji, S., 2002. Chronic stress induces contrasting patterns of dendritic remodeling in hippocampal and amygdaloid neurons. J. Neurosci. 22, 6810–6818.
Weiss, C., Sametsky, E., Sasse, A., Spiess, J., Disterhoft, J.F., 2005. Acute stress facilitates trace eyeblink conditioning in C57BL/6 male mice and increases the excitability of their CA1 pyramidal neurons. Learn. Mem. 12, 138–143.
Weiss, R.D., Martinez-Raga, J., Griffin, M.L., Greenfield, S.F., Hufford, C., 1997. Gender differences in cocaine dependent patients: a 6 month follow-up study. Drug Alcohol Depend. 44, 35–40.
Williams, T.J., Akama, K.T., Knudsen, M.G., McEwen, B.S., Milner, T.A., 2011a. Ovarian hormones influence corticotropin releasing factor receptor colocalization with delta opioid receptors in CA1 pyramidal cell dendrites. Exp. Neurol. 230, 186–196.
Williams, T.J., Milner, T.A., 2011. Delta opioid receptors colocalize with corticotropin releasing factor in hippocampal interneurons. Neuroscience. 179, 9–22.
Williams, T.J., Torres-Reveron, A., Chapleau, J.D., Milner, T.A., 2011b. Hormonal regulation of delta opioid receptor immunoreactivity in interneurons and pyramidal cells in the rat hippocampus. Neurobiol. Learn. Mem. 95, 206–220.
Witter, M.P., 1993. Organization of the entorhinal-hippocampal system: a review of current anatomical data. Hippocampus (3 Suppl.), 33–44.
Xie, C.-W., Lewis, D.V., 1991. Opioid-mediated facilitation of long-term potentiation at the lateral perforant path-dentate granule cell synapse. J. Pharmacol. Exp. Ther. 256, 289–296.